ANALYSIS AND MODELLING OF IMPROVED ACCELERATING CAVITIES FOR THE RECIRCULATING LINEAR ACCELERATOR (RLA)

David L. Smith, Bob N. Turman, and Lawrence F. Bennett
Sandia National Laboratories, Division 1242
P.O.B. 5800, Albuquerque, NM 87185

SAND--90-1677C

DE90 012586

I. ABSTRACT

II. INTRODUCTION
- A. RLA Experiment
- B. ET-2 Cavity Description
  - 1. Accelerator Design Criteria
  - 2. Advantages and Disadvantages
  - 3. Switching Requirements
  - 4. Radial Versus Coaxial Cavities
- C. Goals of New Cavity Design Effort
- D. Typical Circuit Model Description

III. CAVITY MODIFICATIONS
- A. Cavity Trigger System
- B. Accelerating Cavity Performance
- C. Proposed Plastic Liner
- D. Line Three Field Shaper Relocation

IV. NEW CAVITY DESIGN
- A. Circuit Parameter Effects
  - 1. Switch Location
  - 2. REB Loading
  - 3. Transmission Line Impedance
  - 4. Switch Inductance
- B. Symmetric/Split Line Two Alternative

V. CONCLUSIONS

VI. ACKNOWLEDGEMENTS

VII. REFERENCES

ANALYSIS AND MODELLING OF IMPROVED ACCELERATING CAVITIES FOR THE RECIRCULATING LINEAR ACCELERATOR (RLA)

David L. Smith, Bob N. Turman, and Lawrence F. Bennett
Sandia National Laboratories, Division 1242
P.O.B. 5800, Albuquerque, NM 87185

Abstract

By recirculating a relativistic electron beam (REB) in phase with a repeating accelerating voltage, it is possible to construct compact, efficient, high voltage gradient, linear induction accelerators (LIA). Concerns about energy spreads due to degradation of our 1.1-MV, 34-ns duration accelerating cavity repeating pulse shapes have resulted in our improving the 24-switch trigger system for the ET-2[1,2,3] cavity, and identifying critical factors in the cavity design that affect the pulse shape. We summarize the improvements (completed and proposed) for the existing ET-2 cavity pulsed power and the status of our design analysis and modelling for the new four-pass accelerating cavities that could produce a 20-MeV REB for RLA.

Introduction

RLA Experiment

The Recirculating Linear Accelerator at Sandia will transport a 10 to 20-kA injected electron beam guided by an Ionization Front Regime (IFR) plasma channel, which is created with a low energy electron beam (LEEB), through a closed racetrack or a spiral beam line to be re-accelerated by the ringing waveform of dielectric cavities. Figure 1 is a floor plan layout showing the primary components of the RLA concept. By adding more accelerating cavities along the beam line, very significant energies can be rapidly achieved. After being accelerated to the desired final energy, the extracted REB will be available for a number of interesting applications including nuclear effects simulation and hardware vulnerability tests. We have achieved 7-m straight transport and 180° of beam turning with about 94% (peak current) efficiency.[4] Experiments are in progress to diagnose the second 180° turn performance, and the re-acceleration of the beam is to be demonstrated.

We are presently installing a new REB injector for the RLA which will provide a higher amplitude (~4 MV), longer duration (~40-ns FWHM), more rectangularly shaped (~25-ns full width at 90% peak) waveform and a colder beam which will have several advantages over the previous 1.5-MV injector. The more constant beam energy can be more efficiently matched to the guiding IFR plasma channel in the beam line and to the turning section magnetic fields. We are now designing new accelerating cavities that produce more compatible accelerating voltage pulses in terms of waveform flatness, width, and amplitudes that do not suffer unacceptable degradation over the first four ringing periods. This effort requires the application of several network solver and electrostatic field stress analysis computer codes, and eventually a scaled test model to compare actual waveforms to those predicted by the simulations.

ET-2 Cavity Description

A deionized water dielectric, radial cavity based on the ET-2 design has been operating on the RLA. A cross-section of this ET-2 cavity is shown in Fig. 2. The transmission lines were built to maintain a constant impedance to within ±10% for a radially propagating wave. The shape of the outer corner was intended to help compensate for the switch inductance effects. The purpose of the triangular shaped conductors was to keep the output voltage uniformly distributed across the vacuum insulator stack and minimize the peak electric field stress. A simplified model is shown in Fig. 3 where it is compared to an S-3 cavity[5] model. The ET-2 design was chosen as superior because it has a higher gain (2k) and the charged center conductor is removed from the output region. A discussion of the operation and pulsed power requirements of the cavity and RLA was given by Tucker, et al,[6] and a general accelerator conceptual design was described by Hasti, et al.[7] The radial ET-2 line impedances form a ratio of 1:2:6 for line one, line two, and the output line three, respectively. Our existing cavity impedances are about 0.5/1.0/3.0 Ω. The center conductor between line one and line two is first charged to a voltage, V_C. When the switch, located between line one and the output line three, closes, electromagnetic waves are launched into all three transmission lines, and the resulting reflections produce bipolar waveforms at the output terminals of line three. As shown in Fig. 3, the waveform repeats with a period (~136 ns) equal to four times the accelerating pulse duration. The actual accelerating portion should be twice the duration of the one-way transit time, τ, of the transmission lines which are all the same length. When the cavity is operated with a large load impedance mismatch, M, a higher accelerating voltage is produced in return for reduced energy transfer efficiency for each single pass of the electron beam.

Accelerator Design Criteria. The minimum radius of the line three output terminals is determined by the vacuum insulator stack, the configuration of the electrode gap, and the beam drift tube(s) and attached hardware such as solenoidal magnetic field windings, diagnostics, pump ports, etc. The line lengths are determined by the desired output ringing period which must match the recirculation time of the REB. The minimum line separations are limited by both the maximum electric field that the dielectric can maintain and the lower impedance limit when the switches begin to dissipate too much of the stored energy and the switch inductance dominates the pulse shape. The upper limit to the line separations is defined by the reduction of the output voltage due to decreased output impedance mismatch, and also by the subjective point at which the cavity can no longer be considered compact.

The accelerating voltage per ET-2 cavity is given by

$$V_B = 3\ p\ V_C\ (M + 1 - p)\ /\ (M + 1),$$

where p is the number of beam recirculations or passes.[6] The initial impedance mismatch ratio, M, is the effective beam impedance divided by the cavity output impedance. The beam impedance is the accelerating voltage for a given pass divided by the beam current and thus varies from pass to pass. For example, charging our present 3-Ω cavity to 500 kV would produce an ideal output voltage of 1.5 MV. A nominal 10-kA beam current would represent a mismatch of M = 50. Four passes would produce a total acceleration of 5.53 MV, according to the equation.

Advantages and Disadvantages. Dielectric cavities are more attractive than ferromagnetically isolated cavities because of their typically low impedance, light weight, and compactness. Since the ET-2 cavity produces a well defined ringing waveform with an accelerating pulse having an ideal voltage gain of $3V_C$, it is well suited for higher gradient accelerators. A real advantage of using a dielectric cavity is that its poor very-high-frequency response tends to damp out any Beam Break-Up (BBU) instabilities that can arise in the REB. The ringing cavity concept also avoids stringent requirements on high repetition rate switching.

The primary disadvantage of the ET-2 cavity and several others is the resulting bipolar waveform. The additional electrical breakdown stress imposed on the vacuum insulator stack forces present technology designs to stay below 35 kV/cm.[8] The effect of the bipolar waveform on the IFR plasma channel is presently being evaluated to see how it influences the beam guiding and transport.[9] The large number of switches required for this cavity for low inductance operation may be considered a disadvantage also.

Switching Requirements. The present RLA ET-2 cavity is switched by 24 SF_6-filled V/N switches that utilize a capacitively coupled floating trigger disk as seen in Fig. 4.[10] Each switch must carry 25-kA peak current when the cavity is charged to 500 kV. Low jitter, low inductance, reliable operation is required to produce output voltage pulse shapes appropriate for accelerating the current pulse at the proper time. Depending on how many closures actually occur in the multi-channel switches, the overall switch inductance may be 1.5 to 3.0 nH. We expect to continue with this type of switch for the near term until the development of high repetition rate photoconductive (PCSS) or hydrogen gas switch technology evolves.

Radial Versus Coaxial Cavities. An ET-2 cavity that is folded coaxially with respect to the beam line like that of Fig. 5 has obvious size and weight advantages over the radial cavity design. Because it is longer in the axial direction, the accelerating voltage gradient is reduced somewhat when multiple stacked cavities are considered. The electromagnetic waves propagating in the coaxial configuration have the additional corner to negotiate between lines two and three. The corner effects result in output pulse shape distortion if not carefully designed. The outer diameter grows rapidly as the cavity impedance increases, and the size advantage of the coaxial cavity is less significant above about 6 Ω. The geometry allows fewer switches (hence, higher inductance) than for the same impedance radial cavity. So, for lower switch inductance, higher voltage gradients, and minimal corner effects, the radial ET-2 cavity is probably preferable, especially at larger impedances.

New Cavity Design Goals

We are designing new accelerating cavities to provide a high voltage gradient and minimum energy spread in the REB current pulse since the beam uniformity requirements have become even more important for beam quality and transport efficiency purposes, according to theory and simulations, than when the original ET-2 cavity was designed and fabricated. A flat-topped beam is preferred because, when properly timed to match the passing current pulse, all the electrons will be accelerated to the same energy. The new cavities should produce accelerating voltage pulses more compatible with the new 4-MeV, 40-ns injector beam. The desired pulse shapes should be flatter, wider, and have higher successive ringing amplitudes. An example of the pulse shape we are striving toward is given by Fig. 6, which is actually the sum of only the four accelerating pulses simulated by a near ideal circuit model, after they have been time-shifted and overlayed. Before the design and fabrication of new cavities can be completed, we will continue to use the existing cavity on beam turning and recirculation experiments. Thus, modifications are being made on the old cavity to improve its output performance for this intermediate period. The following section addresses some of these changes, both completed and proposed.

Typical Circuit Model Description

A brief summary and explanation of our circuit simulations is deemed useful. The circuit model simulated with the SCEPTRE/ SUPER*SCEPTRE[11] network solving code employs several transmission line models to account for the proper location and dimensions of the hardware in the water dielectric cavity. The switch models are typically a series combination of a time-varying resistor and appropriate inductor which represents the lumped parallel combination of all the cavity switches. The switch is closed by reducing the resistance exponentially with a time constant determined from estimates of the resistive and inductive phase contributions to the switching action.[12] Figure 7 is a circuit schematic for which the SCEPTRE model produces a good match to the actual measured output voltage waveform. The boxes in the figure represent the transmission line models, each with a calculated impedance, Z, and propagation delay time, τ. Resistors without an identifying value are all high impedance monitors. The series L-C circuit on the left side of Fig. 7 represents the lumped Marx generator circuit that charges the cavity lines to about 500 kV in 750 ns. The transmission lines T1, T2, and T3 are the primary cavity lines while all the others represent impedance transitions around corners, junctions, and across interfaces. To provide the cavity model with a realistic load, a current source is added to the output terminals on the right side of the schematic. A Fortran subprogram produces a repeating current pulse defined by the sum of two displaced sine-squared functions. The user then chooses the delay between the current "passes" and the erosion and evaporation rates of the beam to give it a changing character on successive passes. More careful detail can be added to this model, but usually with diminishing returns. Variations of this basic circuit model are used to represent the different cavity modifications which we want to consider.

Cavity Modifications

Cavity Trigger System

Figure 8 is a schematic of the charged-cable switch trigger system we had been using until recently. Due to aging and poor quality control of the silicon rubber-potted isolation capacitors and dc charged coaxial cables, our 24-switch trigger system had degraded to an unacceptable level of repeatability and reliability. Triggering fewer switches resulted in higher inductance operation and asymmetric wave propagation in the radial cavity lines. Considerable diagnostics and circuit model comparisons were necessary to identify the design limitations.

We modified the system to achieve a more reliable switch-triggering performance, as indicated in Fig. 9. We placed all the individual switch isolation capacitors in a common, compact, accessible, oil-dielectric bath eliminating the silicon rubber potting. This potting had voids and damaged regions due to overheating when the coaxial container was sealed. The 70-kV dc charged RG-217/U cables and output pulsed cables were replaced with Dielectric Sciences, Inc. type 2124, 50-Ω cable rated at 100 kVdc. We also installed matching 50-ohm resistors in series with the V/N gas switches at the output ends of the cables. This served to protect the hardware from severe ringing which had been present.

Accelerating Cavity Performance

Primarily as a result of the trigger system modifications the pulsed-power operations have been reliable for hundreds of shots with less than 10% variations in peak voltages. The resulting ET-2 actual waveform of Fig. 10 (solid line) has four well-defined accelerating pulses (the positive going portions) tapering to 50% of the initial 1.1-MV pulse amplitude. It is adequate to accommodate an initial multi-pass recirculating beam experiment. An 8-kA REB load was present for the first pulse only, but did not affect the waveform because of the large impedance mismatch. The waveform simulated by our model is the dotted curve of Fig. 10, which makes a reasonably good fit to the measured data through the fourth accelerating pulse. The ideal waveform included for reference has a period of 140 ns. A 134-ns period would have produced a better phase match with the third and fourth pulses.

Switch triggering statistics over 38 RLA shots have indicated an average switch closure spread of 15.2 ns for ET-2. This corresponds to a one-sigma jitter of 4.9 ns with an average of 21.9 of the switches closing on each shot. Figure 11 shows a polar plot of the accelerating cavity switch timing. The improved performance of ET-2 has helped to achieve 90-100% efficient peak current transport of an 8-kA REB through the first seven-meter straight section of the RLA racetrack. The waveform in Fig. 12 represents the sum of the four simulated accelerating pulses of Fig. 10. As in Fig. 6 the summed voltage pulses forms a good "figure of merit" for comparing circuit performance because it is the total acceleration delivered to a beam making four passes through the cavity. Figure 13 demonstrates how much the summed waveform can change when significant improvements are made to the switch parameters (i.e., the switch inductance and the e-folding closure time were reduced from 1.5 to 1.0 nH and 4.0 to 2.5 ns).

Proposed Plastic Liner

The analytic model for the ideal cavity output is based on abrupt junctions between adjacent transmission lines. A physical cavity, however, must suffer some propagating wave distortion such as at the outer corner of the radial ET-2 where there is the transition between lines one and two. To design an abrupt impedance change at that location is possible, but the conductor shapes could be complicated and/or expensive. We propose to improve our existing cavity by installing a plastic liner against the outermost conductor housing as indicated by the JASON[13] equipotential field plot of the radial cavity in Fig. 14. The purpose of the plastic is to concentrate the electric field (but remain below breakdown stresses) and distribute the energy density around the corner more uniformly. The lower dielectric constant means faster wave propagation, and the plastic should suppress higher order modes during the ringing.[14] Picturing the plastic in terms of a transmission line in parallel with the water transmission line around the corner, but with a shorter propagation delay time, one can expect the outer portion of the wave front making the turn to be able to keep up with the inner portion, which travels a shorter distance in water. The design trade-off involves using as thick a liner as possible to minimize the transition effects while not exceeding electric field breakdown stresses in the plastic or on the plastic/water interface. The 2-cm thick liner of Fig. 14 sees about one-half the 500-kV charge voltage or about 125 kV/cm at the highest stressed point. The effect of a near ideal corner on the 3-Ω ET-2 cavity is shown by Fig. 15 and also by the summed wave shape of Fig. 16. We plan to try this improvement to the cavity in the very near future.

Line Three Field Shaper Relocation

The triangular shaped conductors in the radial ET-2 cavity 3-Ω output line three (Figs. 2 & 14) are field shapers which serve to maintain constant impedance for the radially travelling waves. A subjective inspection shows the junction between line two and line three to be properly symmetric. However, line one is offset sufficiently to one side that interacting waves between it and line three must undergo some distortion due to the asymmetry and wave propagation time delays. If the results of our analytical evaluation[14] indicate further study is warranted, a 3-D computer analysis may be pursued to examine the degree of this problem. Possible solutions that we are considering include removing the field shapers and tapering the outside conductor surfaces to maintain a constant impedance, single line. Future cavity designs may avoid this issue if we choose something like the symmetric/split line two configuration discussed later.

New Cavity Design

Circuit Parameter Effects

Our recent ET-2 circuit model study has helped to determine the primary factors causing the voltage amplitude loss in the repeating waveforms. We are following up these preliminary results with a design effort to include corrections in the new cavity hardware. Switch inductance, resistance, and precise location of the switch hardware can all have significant impacts on the pulse shapes and amplitudes. The simulated waveform of Fig. 9 was achieved by using an overall switch inductance of 1.5 nH and a 4.0-ns e-folding closure time. Reducing the switch inductance, and to a lesser extent the resistance, tends to improve accelerating pulse rise times and peak values. The exact position of the cavity switches can affect the wave shape significantly. Other important parameters that affect the waveform are the REB loading effect on the cavity and the actual cavity impedance. We expand on these effects in the following discussion.

Switch Location. Because of the finite size of the V/N spark gap switches and mechanical mounting requirements, the present cavity switch locations are not placed exactly on the junction between lines one and three. Increasing the effective length of line one (see Fig. 2) by moving the switch position 7.5 cm radially inward has resulted in raising the simulated amplitudes of the latter accelerating pulses. Figure 17 demonstrates this effect with the improved waveform generated by a switch position modification of the circuit in Fig. 7. Also shown in Fig. 17 is the modelled beam current load in phase with the accelerating pulses. The peak current is allowed to reduce from 13 kA to 10 kA in four cycles.

REB Loading. As the circuit load mismatch is reduced the effect of the REB current on the pulse shape becomes more pronounced. The effect of REB loading on the 3-Ω ET-2 waveform is shown in Fig. 18. Although the impact is not severe on the first two pulses, it is more apparent on the third and fourth. The mismatch varies directly with the accelerating voltage and inversely with the beam current and the cavity output line impedance.

Transmission Line Impedance. To get a handle on the output voltage sensitivity to the transmission line impedance, we varied the line impedance combinations from 0.5/1.0/3.0 Ω to 1.5/3.0/9.0 Ω while holding constant other circuit parameters. These models included an ideal corner, REB loading, and a switch inductance of 1.5 nH. The switch closing time was allowed to vary slightly due to the changing impedance which it had to drive. One method of presenting the results is demonstrated in Fig. 19 where we plot the sum of the four accelerating voltage peaks against the cavity output line impedance and compare it to the case of the unloaded (open) circuit model. For the unloaded case the large mismatch allows the output to continue increasing with cavity impedance, but the effect of a beam load tends to turn the total voltage back down after an optimum at about 6 or 7 Ω. To account for the different accelerating pulse shapes we plot in Fig. 20 the total energy added to the four-pass beam current as a function of the output line impedance. The results still show a similar design range for optimum cavity performance. Higher cavity impedance is also less demanding on the switches. As the output line impedance was varied from 3 to 6 to 9 Ω, the total energy dissipated by the switches reduced from 39% to 19% to 11%, respectively.

Switch Inductance. The switch inductance is generally accepted as being a critical parameter in defining a desirable waveform. We find the switch inductance affects the rise time, amplitude, and phase of the ringing waveform as shown in Fig. 21, where the inductance is varied from 0.75 to 3.0 nH for a 3-Ω ET-2 model with the same REB load, a plastic corner, and an e-folding switch closing time constant of 4 ns. The 1.5 to 2.0 nH range looks preferable to either lower or higher inductances. This probably is explained by a preferred ringing period that better matches the cavity line lengths. Figure 22 is a plot of the summed four voltage peaks versus the effective switch inductance. The curve for the 3-Ω cavity cases clearly shows an optimum in the 1.5 to 2.0-nH range, but the 6-Ω cavity curve continues to improve with reduced inductance. In terms of total energy added to the four-pass beam as a function of the switch inductance, Fig. 23 supports the same conclusion.

Symmetric/Split Line Two Alternative

To apply what we have learned thus far from our operating experience with the 3-Ω ET-2 and the results of the preliminary modelling effort, we are evolving toward some new cavity design concepts. As one of several options available to us, the cross-section of the radial cavity in Fig. 24 demonstrates these concepts. It is a 1/2/6-Ω cavity, except line two is split and located on both sides of line one to provide the maximum symmetry and communication with line three. Even though a little larger, the 6-Ω cavity models have indicated an accelerating pulse performance advantage over 3 and 9-Ω cavities with respect to REB loading and switch inductance effects. The 17-ns transmission line lengths are only slightly longer than the existing cavity lines, so it could be a direct replacement. The low-inductance switches should be mounted as far radially inward as mechanical stability allows, and the maximum number allowed by the radial geometry should be installed. The outermost corners which the propagating electromagnetic waves have to negotiate may or may not require a plastic liner depending on how abruptly the transition is made with respect to the line lengths. In addition, as the waves turn around the dual corners in opposite directions, the symmetry effects may add to compensate for wave front distortion.

The conceptual cavity of Fig. 24 does force some operational complications which have to be considered. Access to the switches for routine maintenance is indeed hindered. Fill and purge gas lines and trigger cables (or fiber optics) will have to be protected. Two charging voltages of opposite polarity are required, but at half the total voltage which reduces electrical stress requirements in the dielectric and at the corners. Regardless of our final decision for a new cavity design, each will have similar pros and cons that have to be weighed carefully.

Conclusions

The ET-2 accelerating cavity has performed well with the switch trigger system improvements. Possible modifications to the ET-2 design to produce more flat-topped and more constant amplitude repeating pulse shapes are going to be pursued. Our simulated parameter survey has indicated several circuit operating point goals on which to base the new accelerating cavity designs. The combination of the new injector and improved accelerating cavities will provide a desirable higher-γ electron beam to accomplish recirculation and re-acceleration milestones on the RLA.

Acknowledgements

This work was funded by DOE under contract DE-ACO4-76DPOO789 and by Navy SPAWAR under SPACETASK No. 145-SNL-1-8-1. Special thanks are in order for Samuel Lucero, of Diversus, Inc., who was our primary accelerator operator, performed both routine and non-routine maintenance, and provided excellent trouble-shooting support. Bill Tucker and Ken Prestwich deserve our gratitude for their earlier design efforts upon which this work is based. We do appreciate the suggestions concerning field shapers and plastic inserts from Bill Johnson, who is participating in the cavity design analysis.

References

1. D. Ecclechall and J. K. Temperly, J. Appl. Phys. 49, 1981, p. 3649.
2. D. Ecclechall and C. E. Hollandsworth, IEEE Trans. on Nucl. Sci. 28, 1981, p. 3386.
3. I. D. Smith, Rev. Sci. Instrum. 50, 1979, p.714.
4. Private Communications with Bob Platt, SAIC, Albuquerque, NM, May 1990.
5. I. D. Smith, Sandia Report No. SAND79-7043, Sandia National Labs, Albuquerque, NM, May 1979.

6. W. K. Tucker, et al., Proc. Sixth IEEE Pulsed Power Conf., Arlington, VA, IEEE Cat. No. 87CH2522-1, June 1987, p. 470.
7. D. E. Hasti, et al., Sandia Report No. SAND87-0150 UC-28, Sandia National Labs, Albuquerque, NM, June 1987.
8. W. K. Tucker, et al., Proc. Fifth IEEE Pulsed Power Conf., Arlington, VA, IEEE Cat. No. 85C2121-2, June 1985, p. 323.
9. Private Communications with Mike Mazarakis, Sandia National Labs, Albuquerque, NM, Apr 1990.
10. W. K. Tucker, Sandia Report No. SAND82-1183, Sandia National Labs, Albuquerque, NM, July 1982.
11. J. C. Bowers and S. R. Sedore, "SCEPTRE: A Computer Program for Circuit and System Analysis," Englewood Cliffs, NJ, Prentice Hall, 1971.
12. J. P. VanDevender and T. H. Martin, IEEE Trans. on Nucl. Sci. 22, No. 3, p. 979, June 1975.
13. S. J. Sackett, "JASON-A Code for Solving General Electrostatics Problems, User's Manual," CID-17814, LLL, Livermore, CA, 1978.
14. Private Communications with Bill Johnson, Sandia National Labs, Albuquerque, NM, May 1990.

FIGURE CAPTIONS

Fig. 1. Floor plan of the RLA.

Fig. 2. Radial ET-2 cross-section.

Fig. 3. Models and waveforms of the ET-2 and S-3 cavities.

Fig. 4. The ET-2 V/N spark gap.

Fig. 5. The coaxial ET-2 configuration.

Fig. 6. Summed accelerating pulses for a near ideal 6-Ω ET-2 model with beam loading.

Fig. 7. Simplified circuit model for the existing 3-Ω ET-2 cavity.

Fig. 8. Previous switch trigger system.

Fig. 9. Present switch trigger system.

Fig. 10. Measured, simulated, and ideal 3-Ω ET-2 waveforms.

RLA FLOOR PLAN FOR ON-AXIS INJECTOR

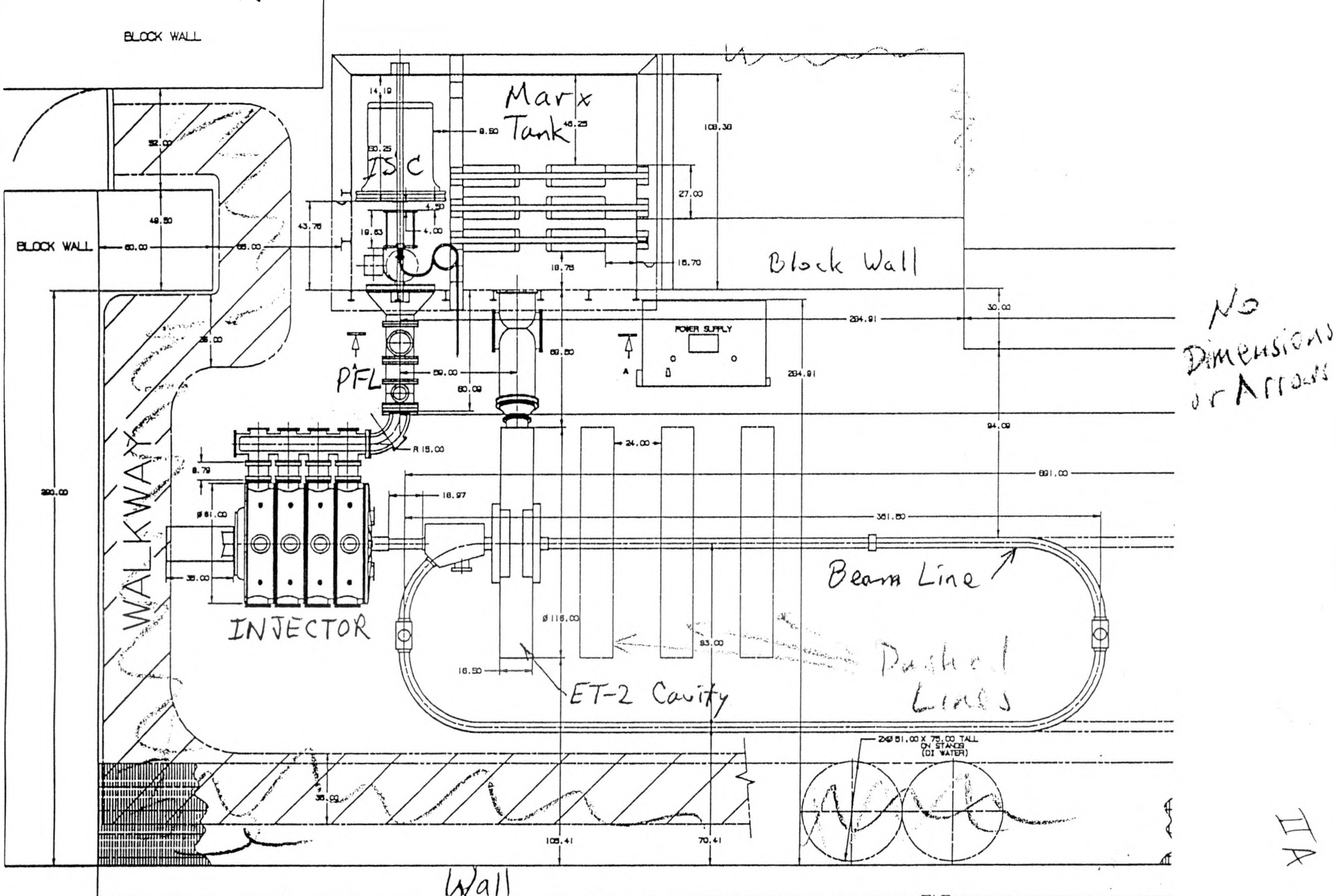

Fig. 1

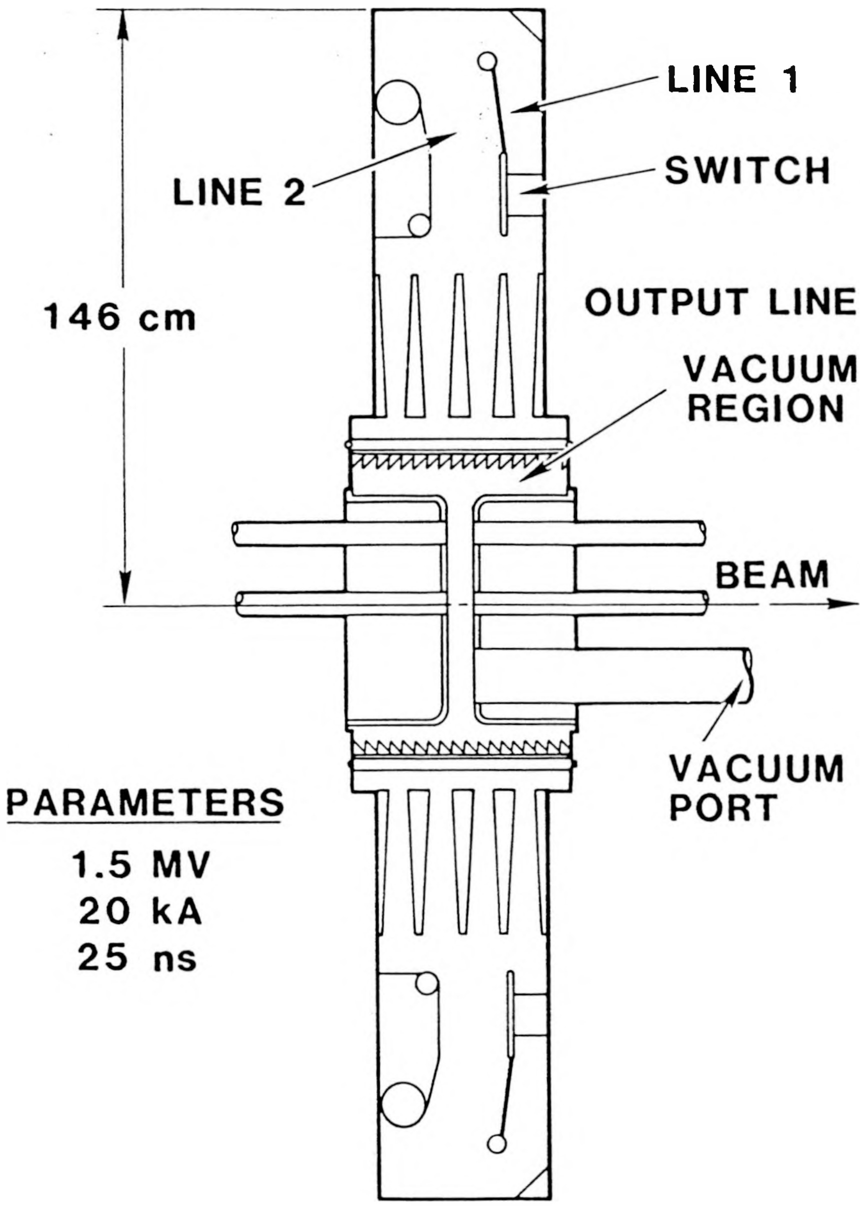
LINE 1
LINE 2
SWITCH
146 cm
OUTPUT LINE
VACUUM
REGION
BEAM
VACUUM
PORT
PARAMETERS
1.5 MV
20 kA
25 ns

Fig. 2

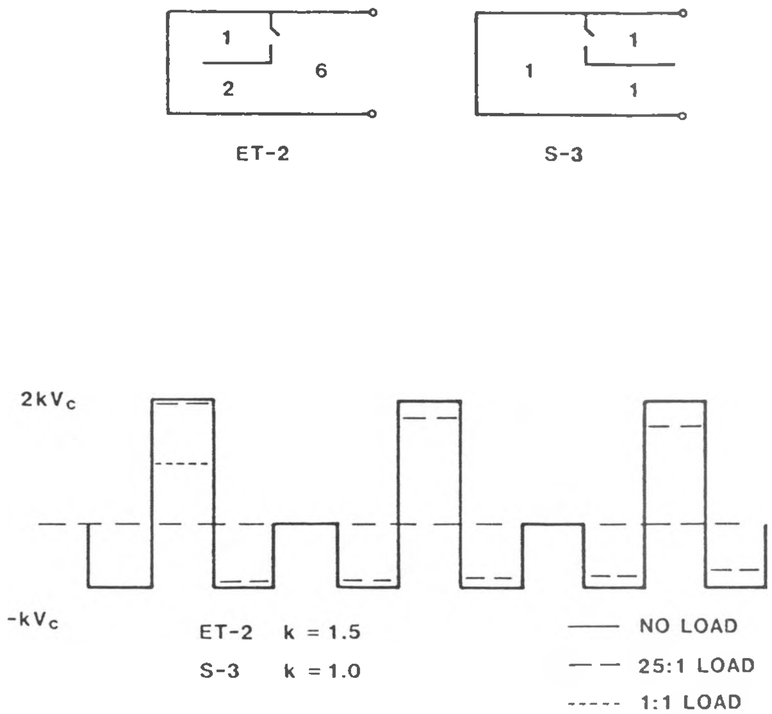

Fig. 3.

V/N SPARK GAP

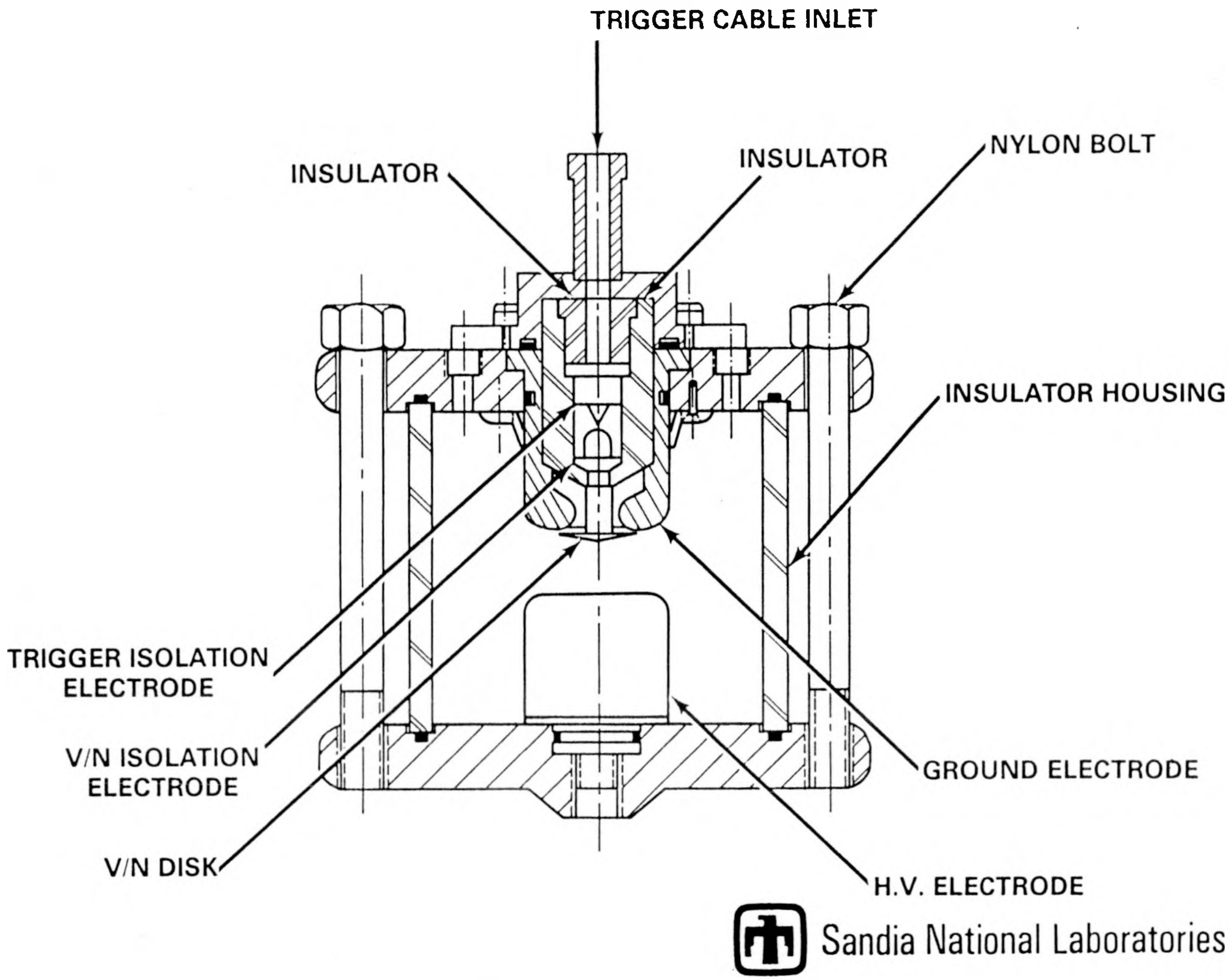

Fig. 4

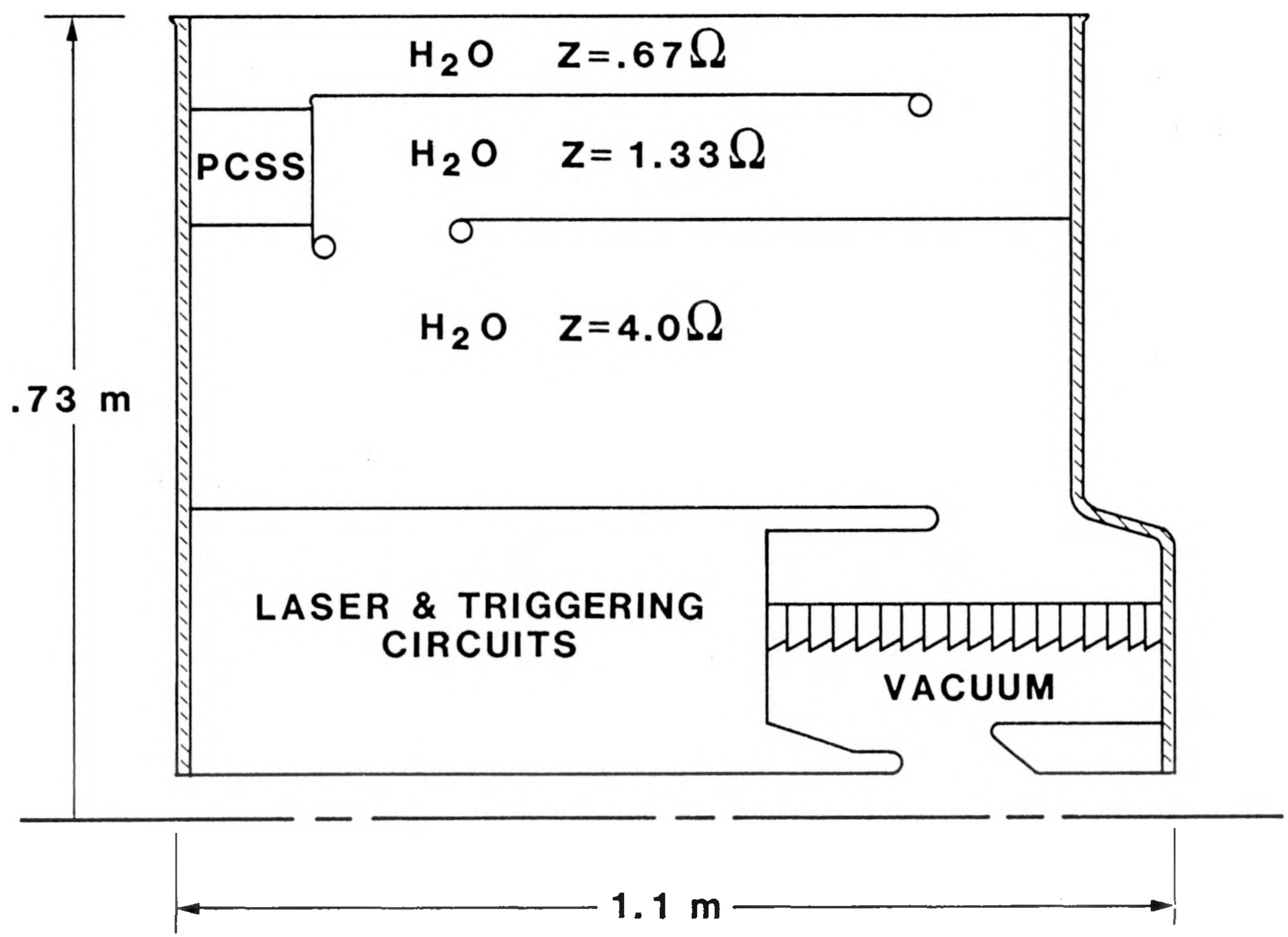

H2O Z=.67Ω
PCSS
H2O Z= 1.33Ω
H2O Z=4.0Ω
.73 m
LASER & TRIGGERING CIRCUITS
VACUUM
1.1 m

Fig. 5

5/17/90 9:42:50
SWS7RB

SUMMED ACCELERATING PULSES FOR NEAR IDEAL 6-Ω ET-2 MODEL WITH BEAM LOADING

(10)

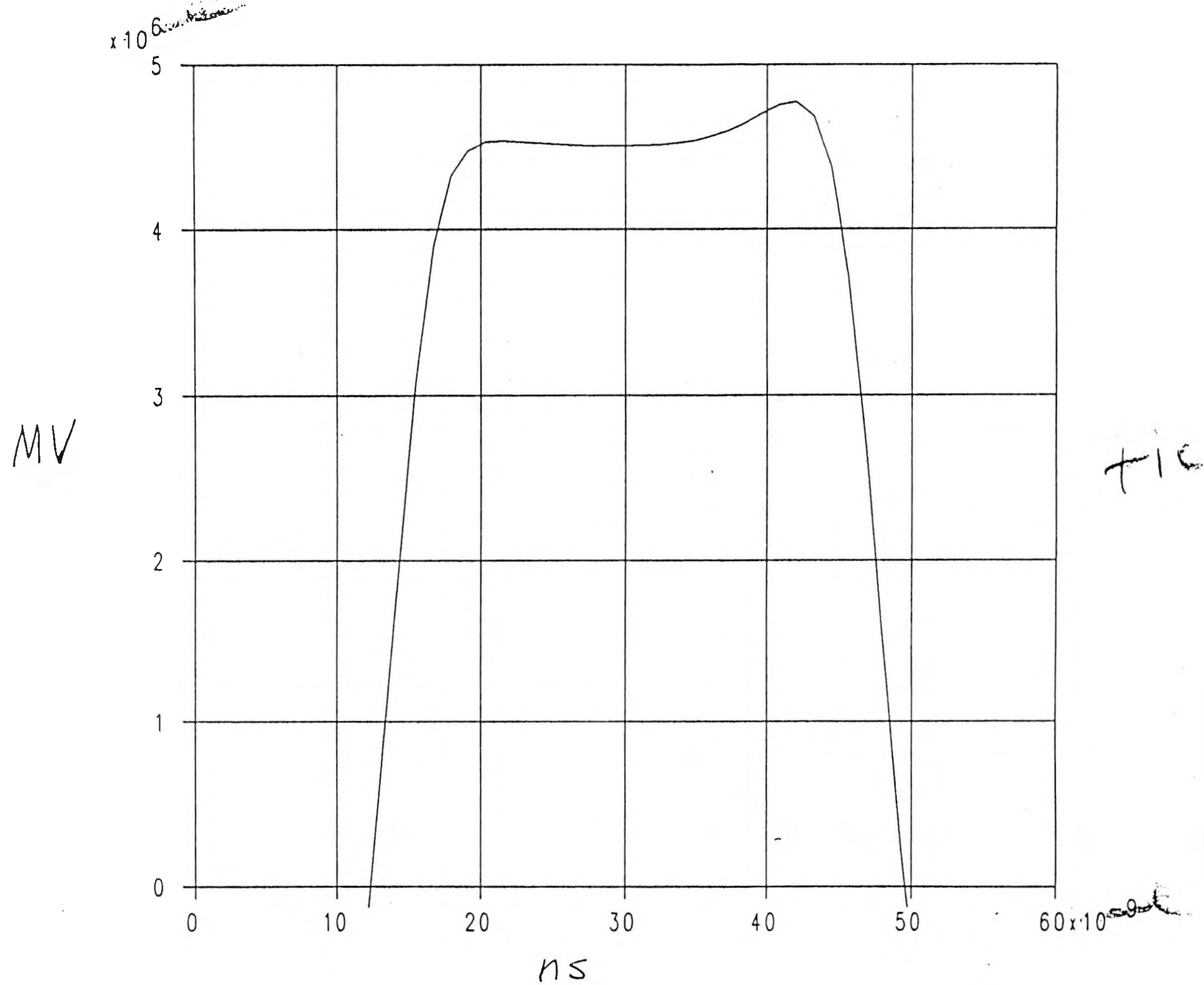

Fig. 6

DETAILED CIRCUIT MODEL FOR EXISTING 3-Ω ET-2

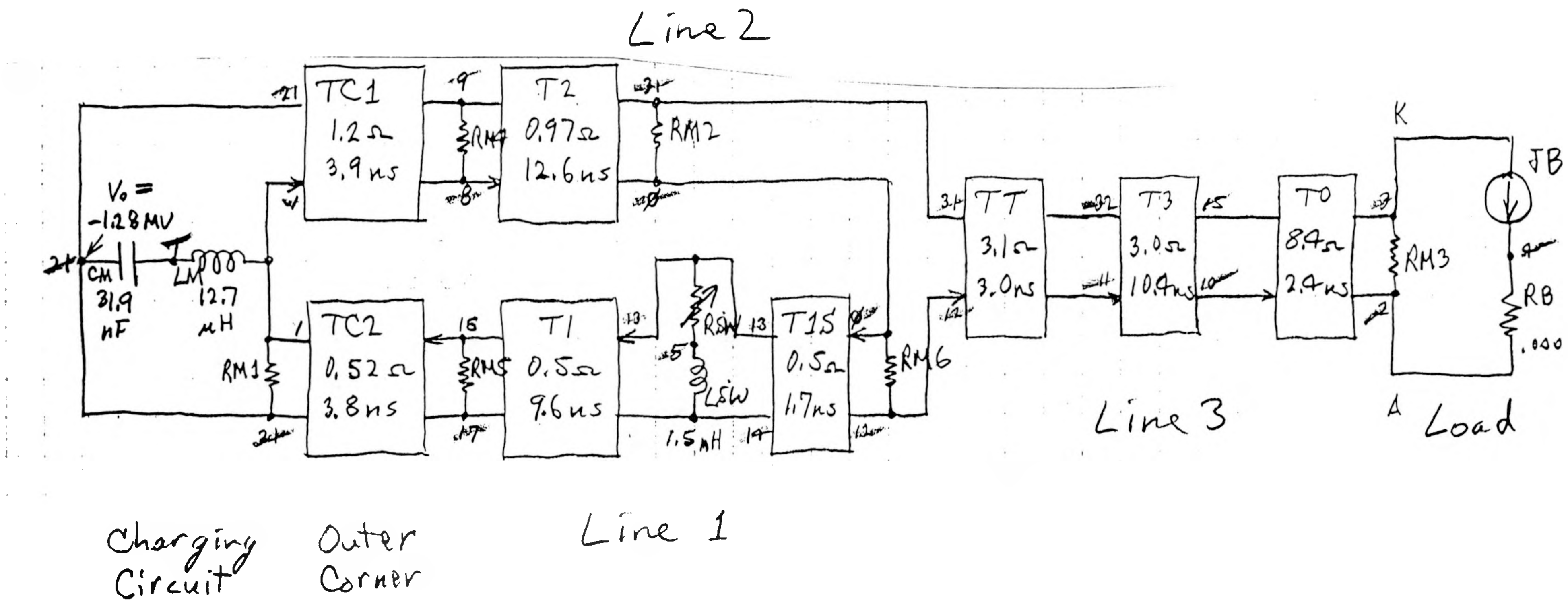

Fig. 7

RLA SWITCH TRIGGER SYSTEM
FIRST MODIFICATION

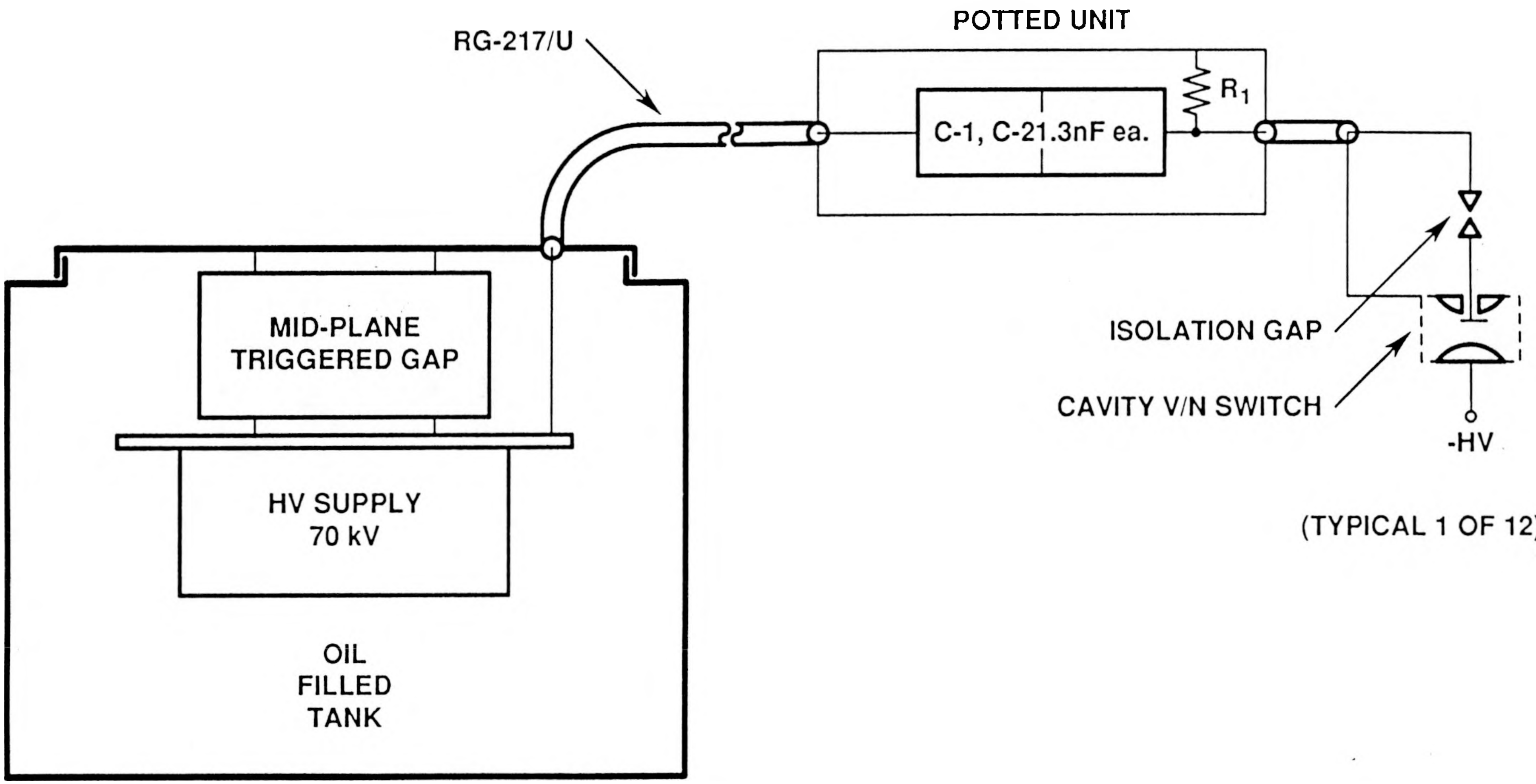

Fig. 8

TA0049.02.09

RLA SWITCH TRIGGER SYSTEM
PRESENT CONFIGURATION

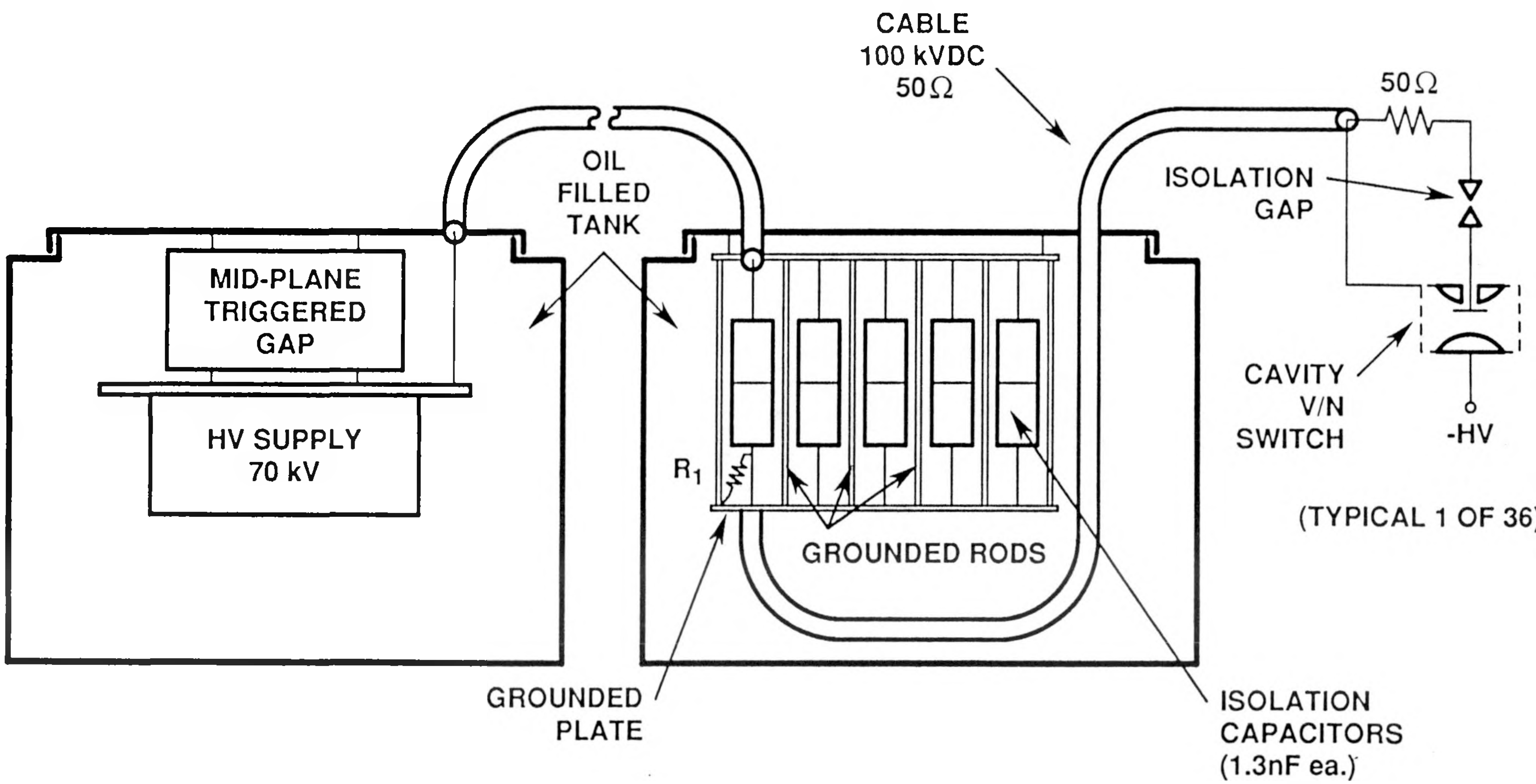

Fig. 9

TA0049.02.10

ACTUAL, SIMULATED, AND IDEAL ET-2 WAVEFORMS

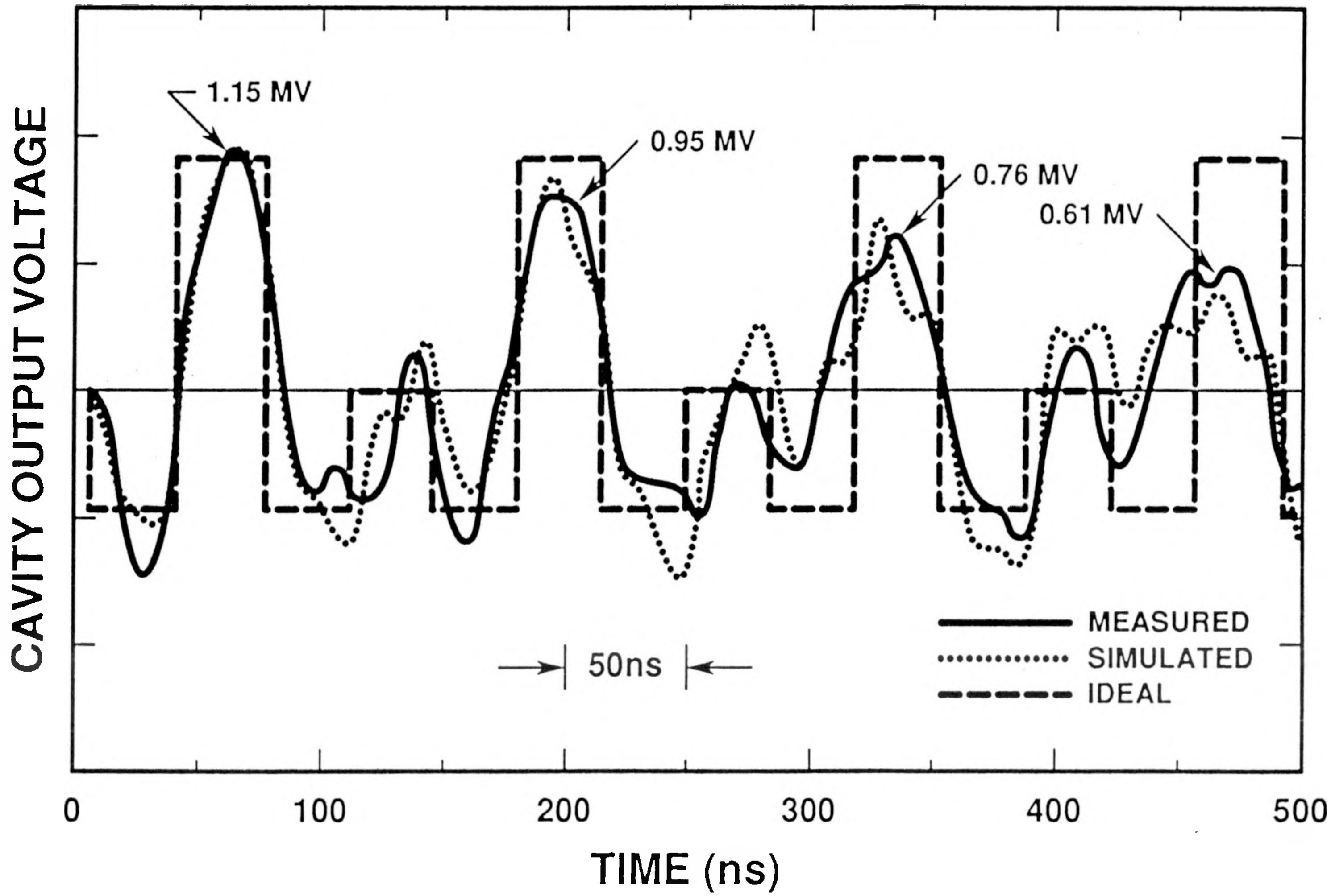

Fig. 10

TA0049.02.05

ET-2 SWITCH TIMING vs. POSITION

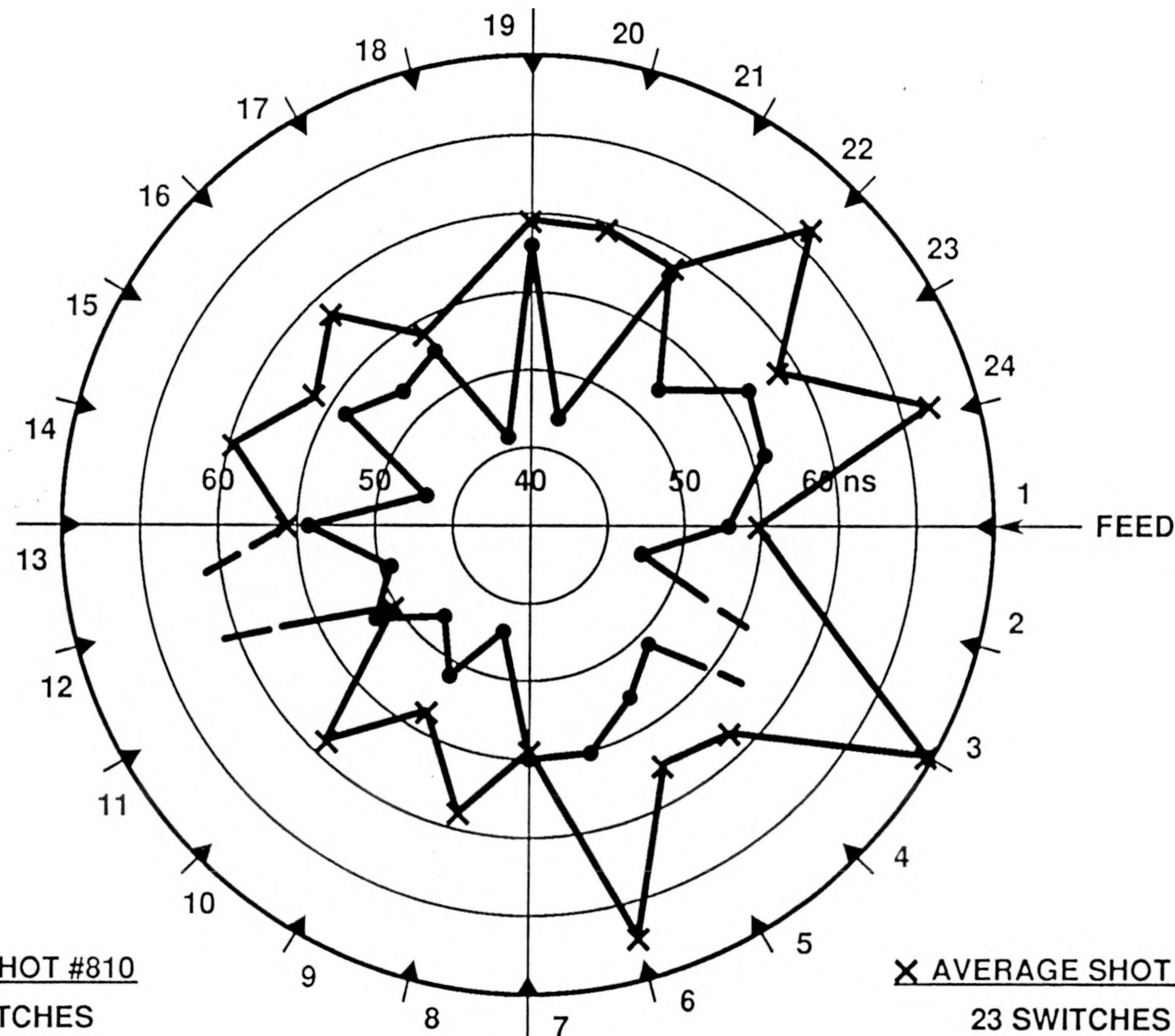

● BEST SHOT #810

23 SWITCHES
12.7ns SPREAD
3.9ns JITTER

X AVERAGE SHOT #819

23 SWITCHES
15.2ns SPREAD
4.9ns JITTER

Fig. 11

TA0049.02.06

4/25/89 15:25:47
ET2ACTUAL4

SUMMED ACCELERATING PULSES (SIMULATED)

FOR EXISTING 3-Ω ET-2

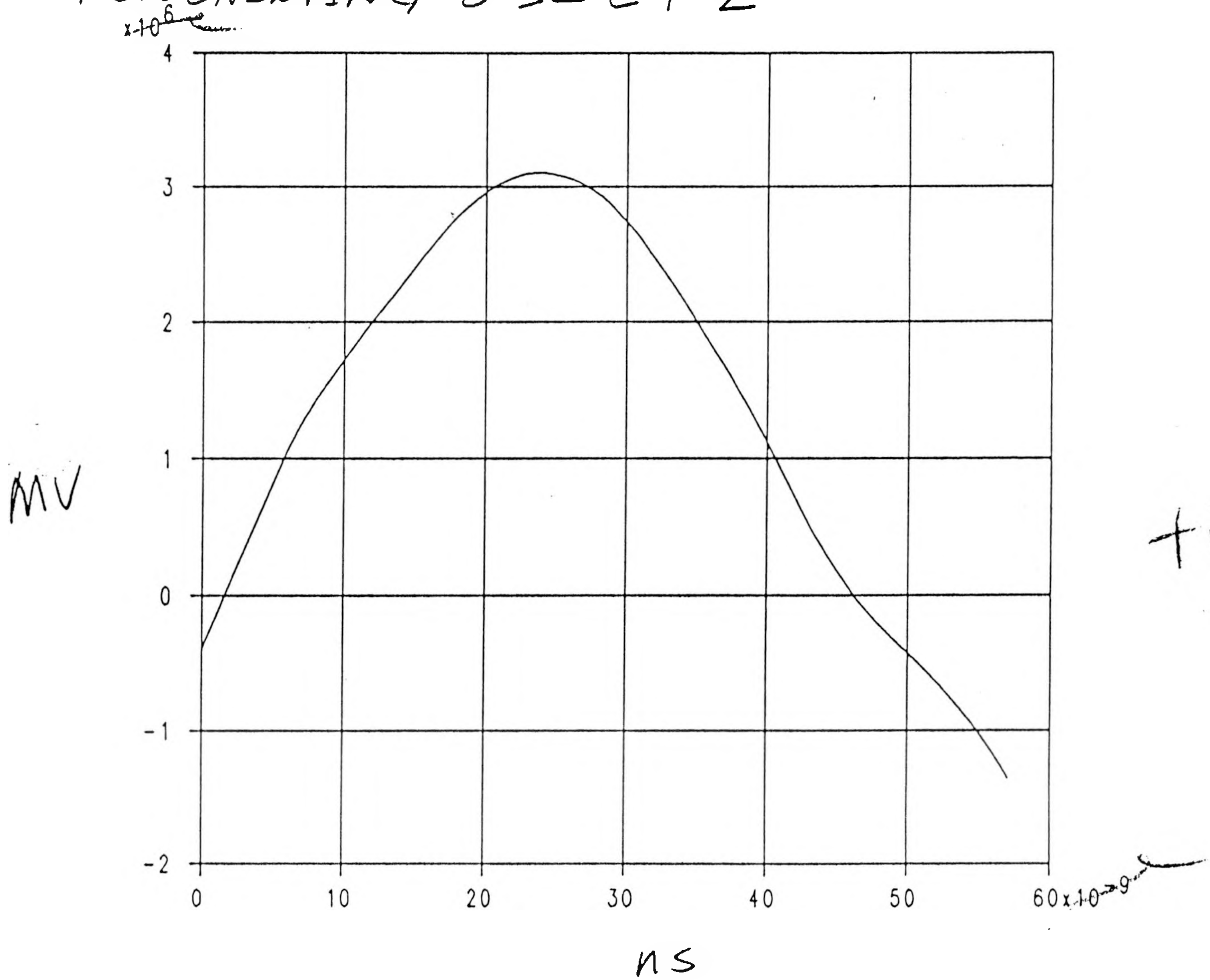

Fig. 12

III B

4/26/89 15:03:40
ET2ACTUAL2

SUMMED ACCELERATING PULSES (SIMULATED)

Improved Switch Parameters, 3-Ω ET-2

1.5 → 1.0 nH Lsw
4.0 → 2.5 ns τ

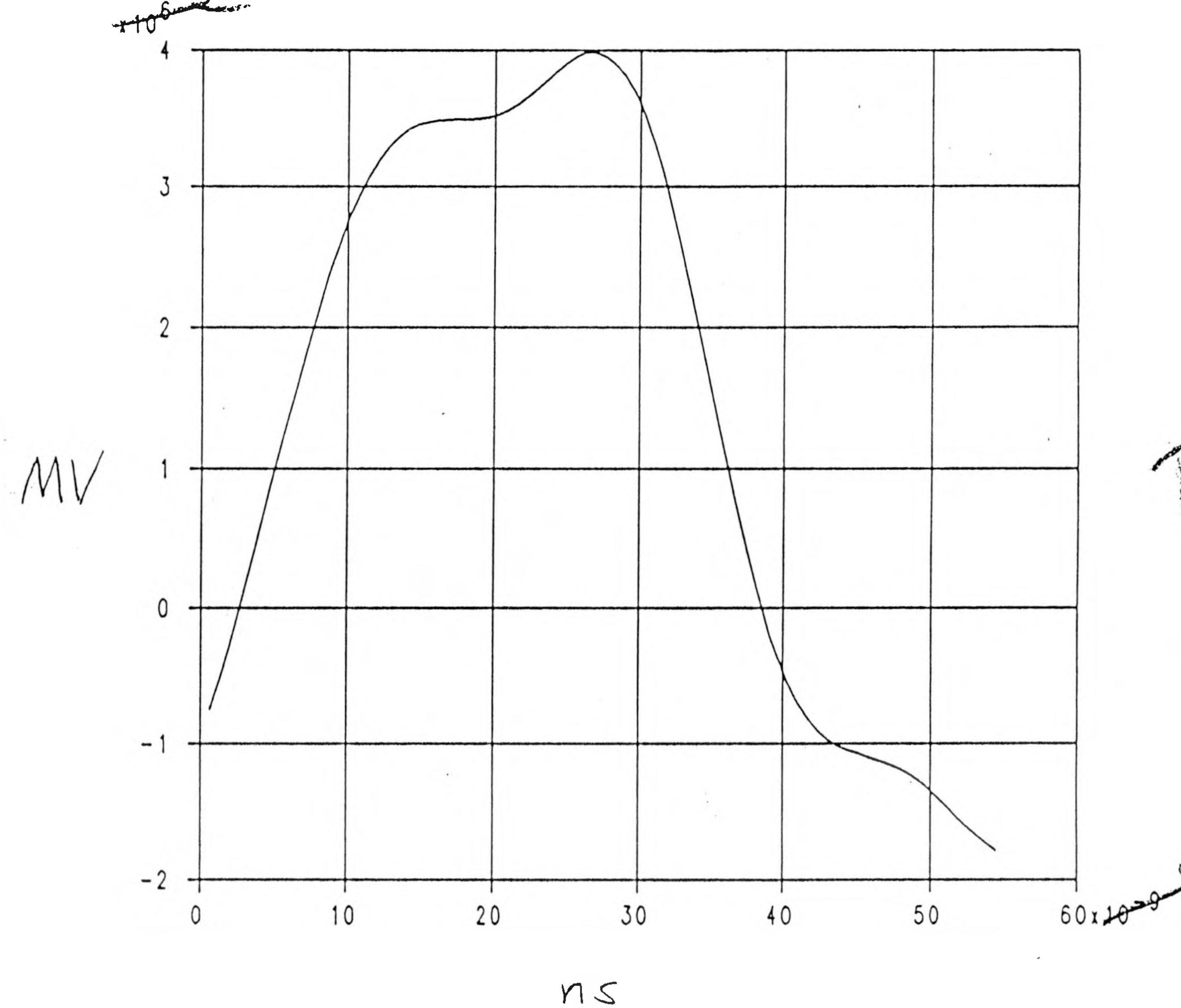

Fig. 13

EQUIPOTENTIAL PLOT FOR THE CHARGED RLA ET-2 CAVITY WITH PLASTIC LINER

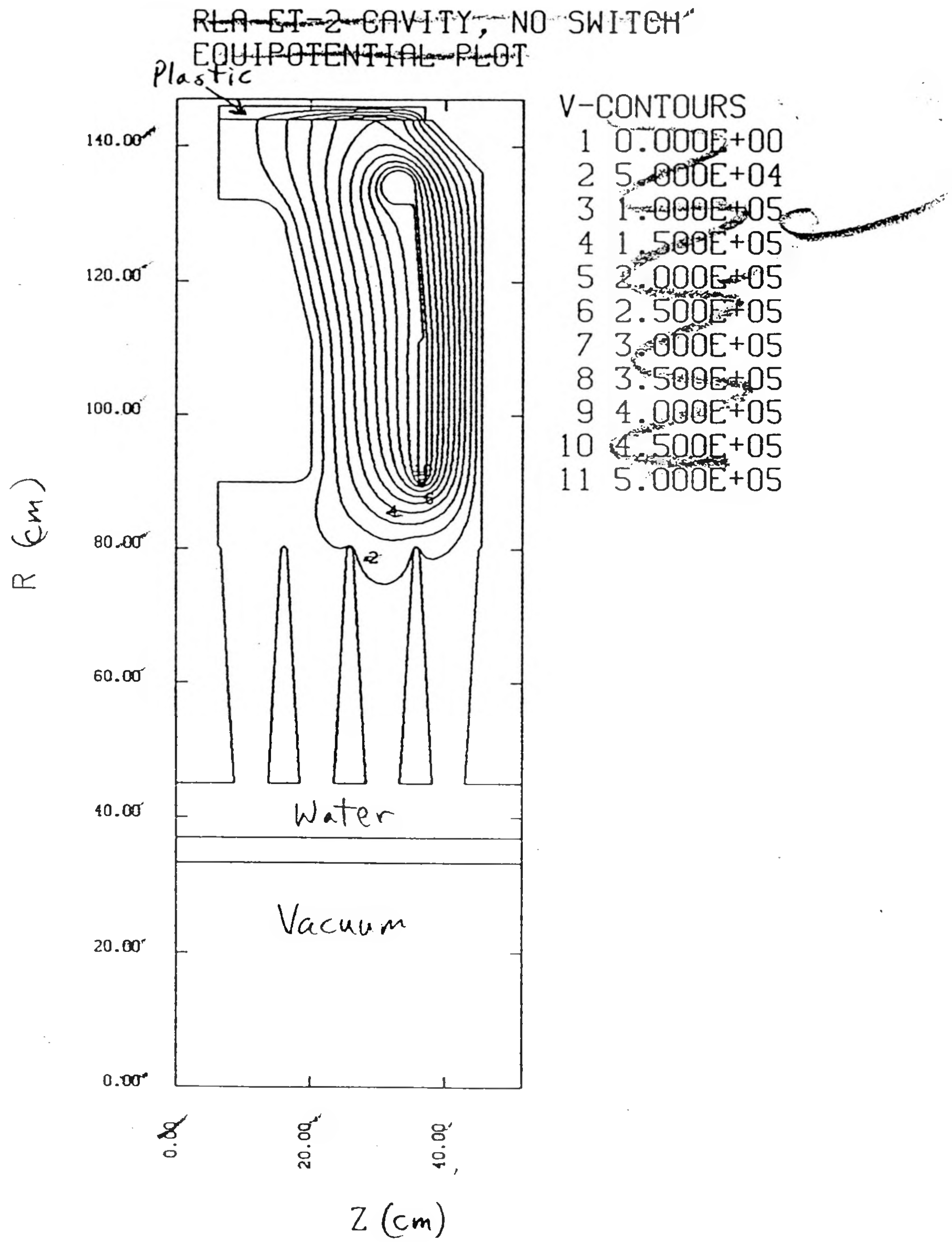

Fig. 1A

BEST SIMULATION FOR EXISTING ET-2 CAVITY

WITH AND WITHOUT PLASTIC ADDED TO THE CORNER

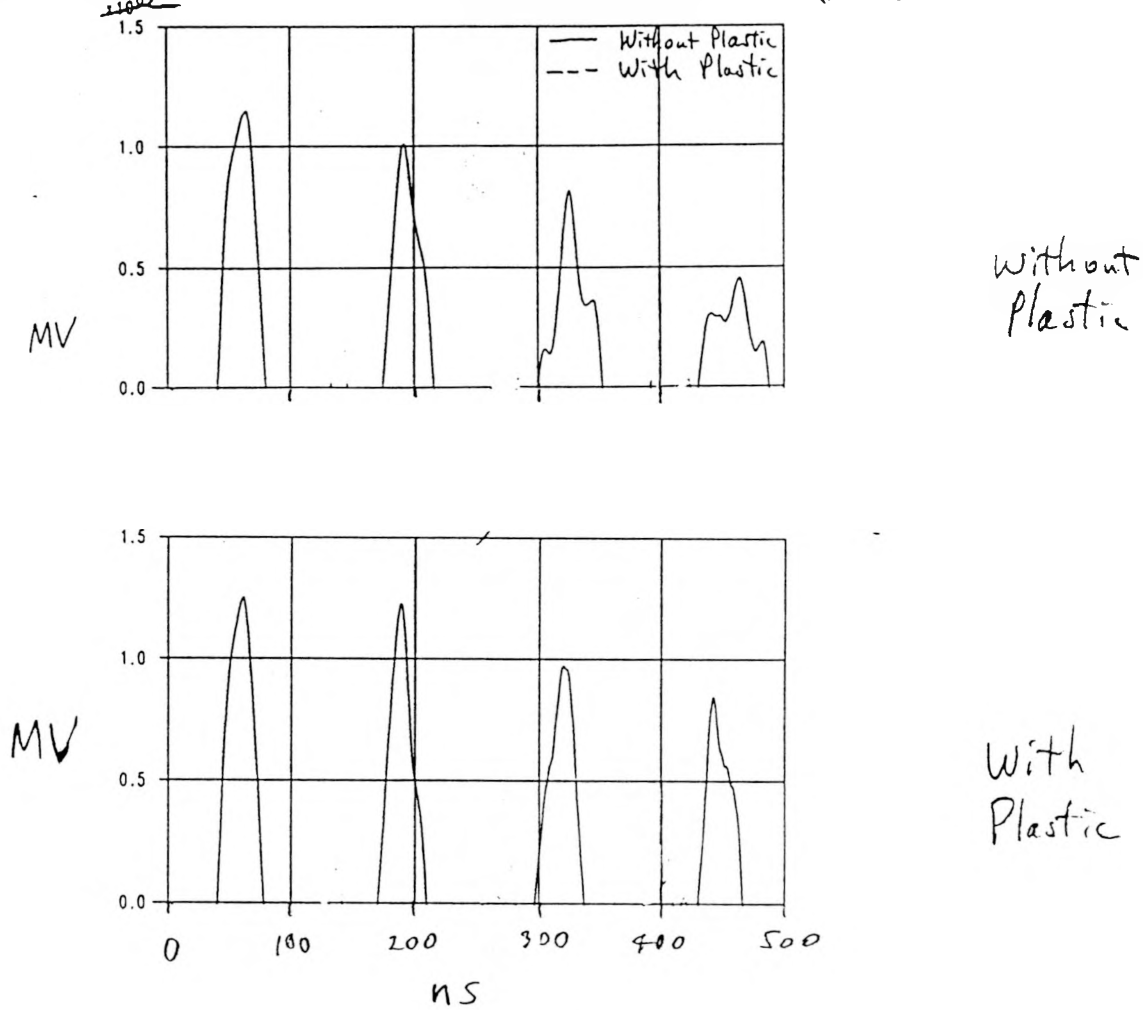

These will be overlayed

Fig. 15

2/ 2/90 13:53:41
ET2ACT4PL1RBM

SUM OF SUCCESSIVE ACCELERATING WAVEFORMS

(Modified Corner, ~~500-kV, Half-Length~~ 3-Ω ET-2)

Max charge
Near Ideal Corner

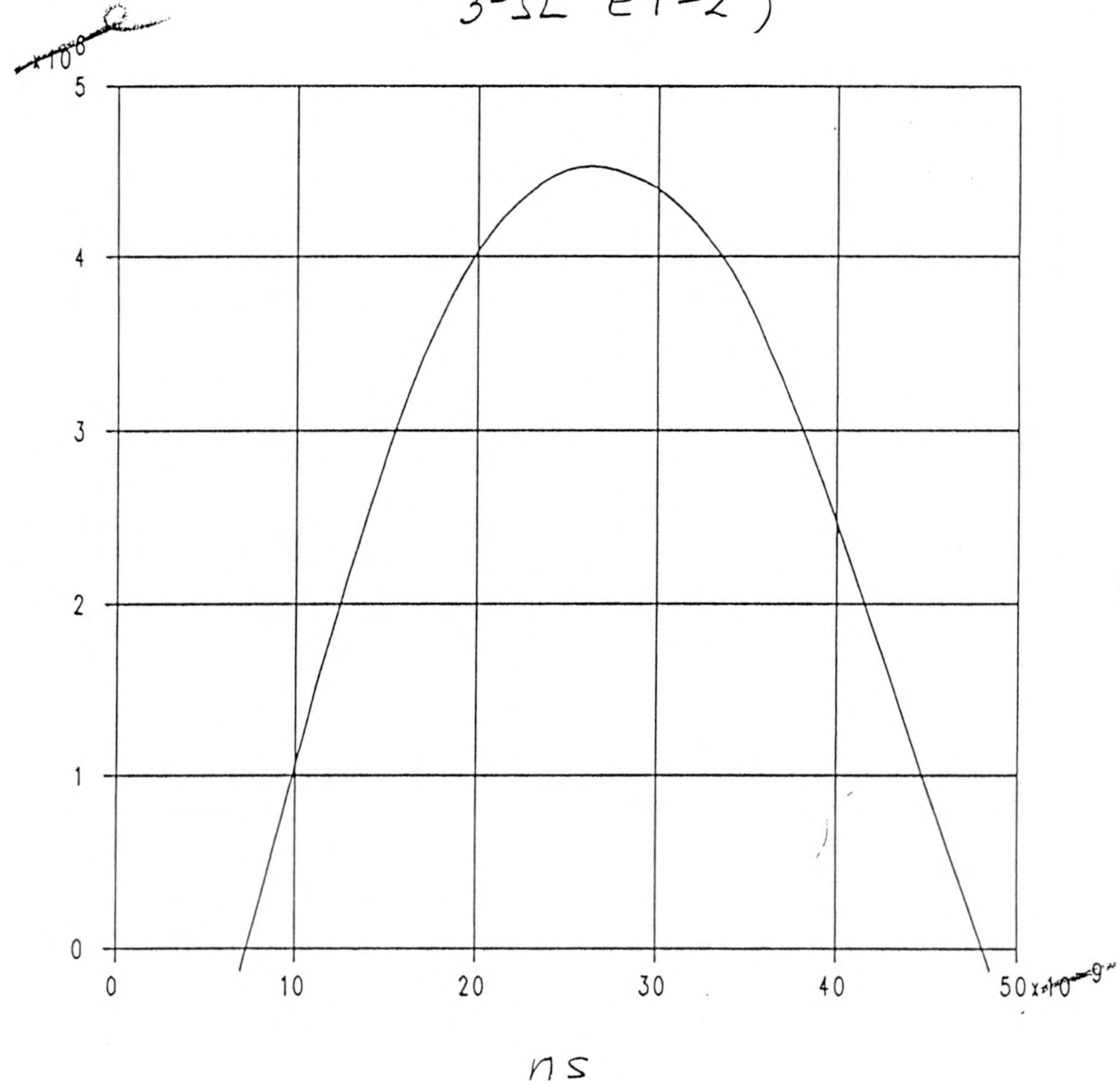

Fig. 15

~~ΣVpk 4.16MV for Vch = 500kV~~ ~~ETCAV4~~ ~~(Switch at end of Line 1)~~

BEAM CURRENT AND 3-Ω ET-2 OUTPUT VOLTAGE FOR CASE OF SWITCH LOCATED AT THE EDGE OF LINE 1

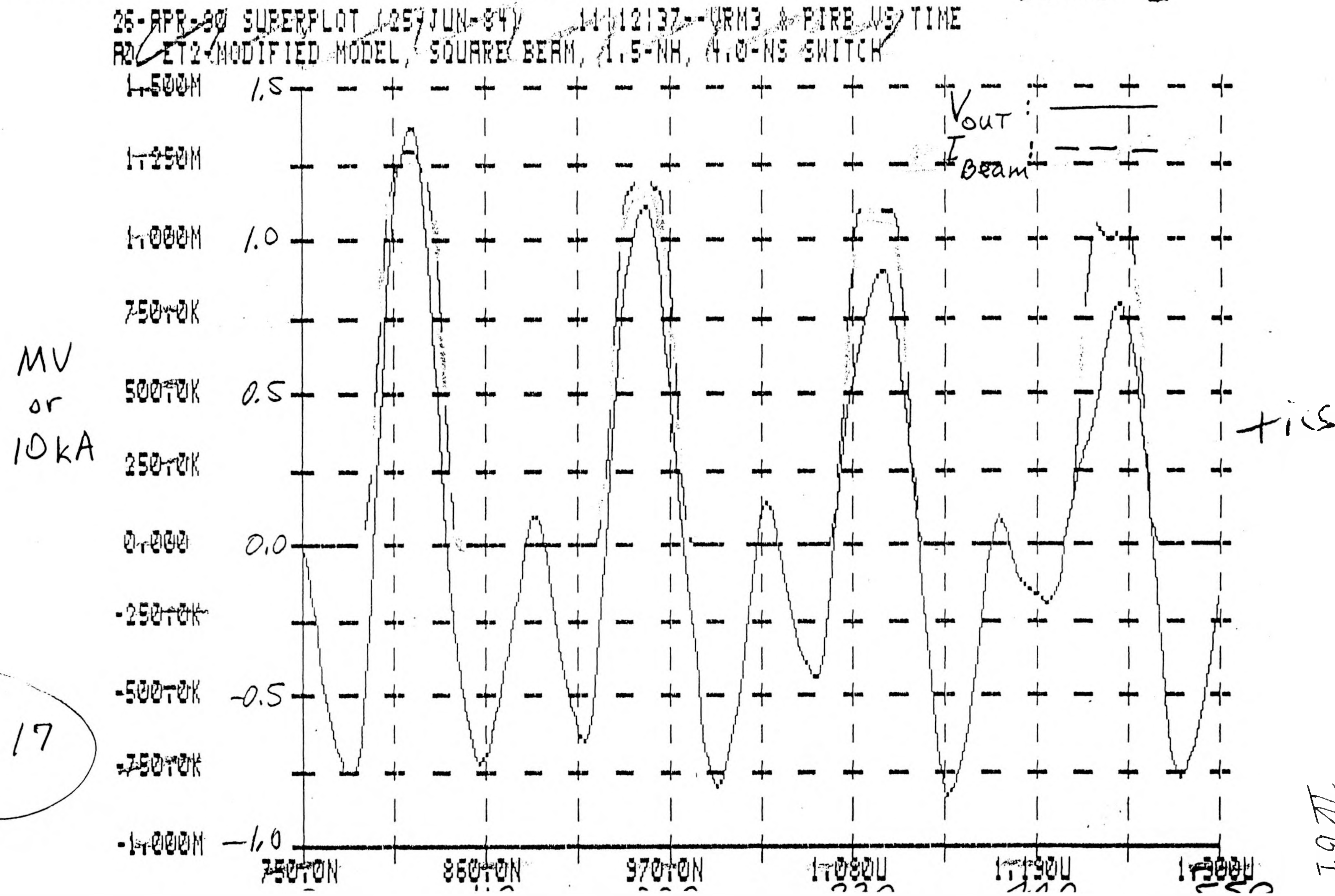

Fig. 17

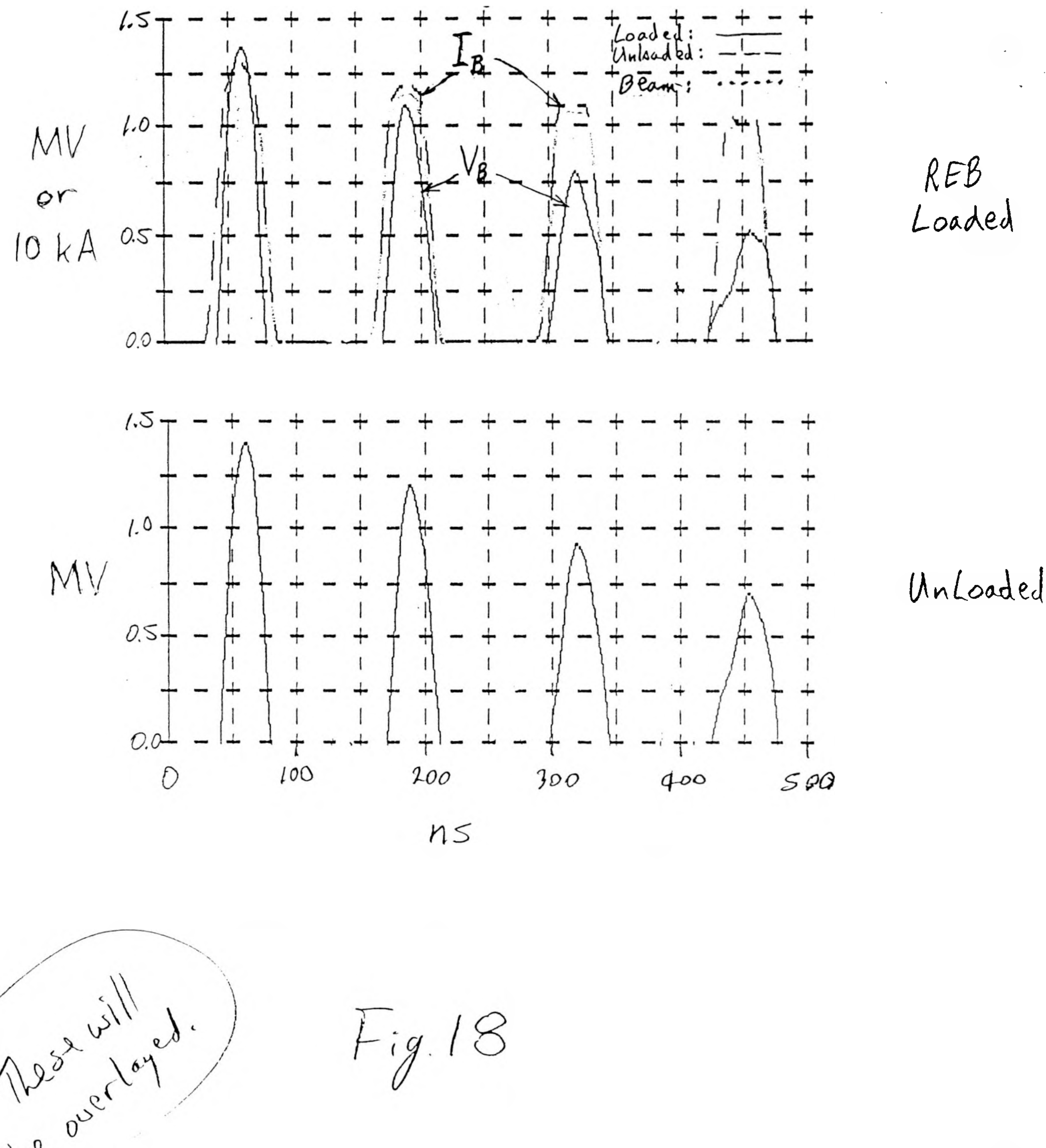

1.5
1.0
0.5
0.0
MV
or
10 kA
Loaded:
Unloaded:
Beam:
I_B
V_B
REB
Loaded
MV
UnLoaded
0
100
200
300
400
500
ns
These will be overlayed.

Fig. 18

5/29/90 8:30:30

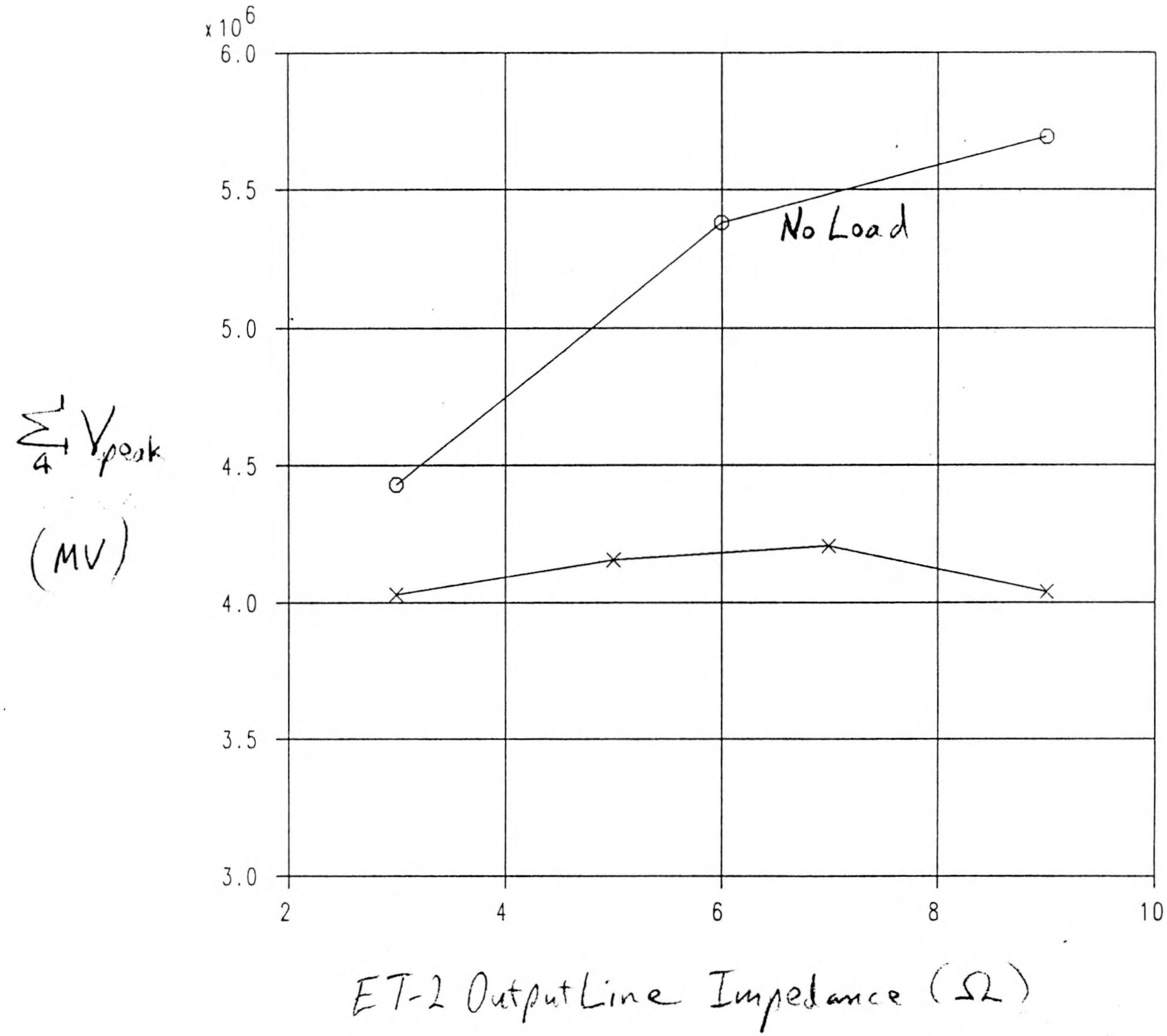

Fig. 19

5/29/90 8:32:28

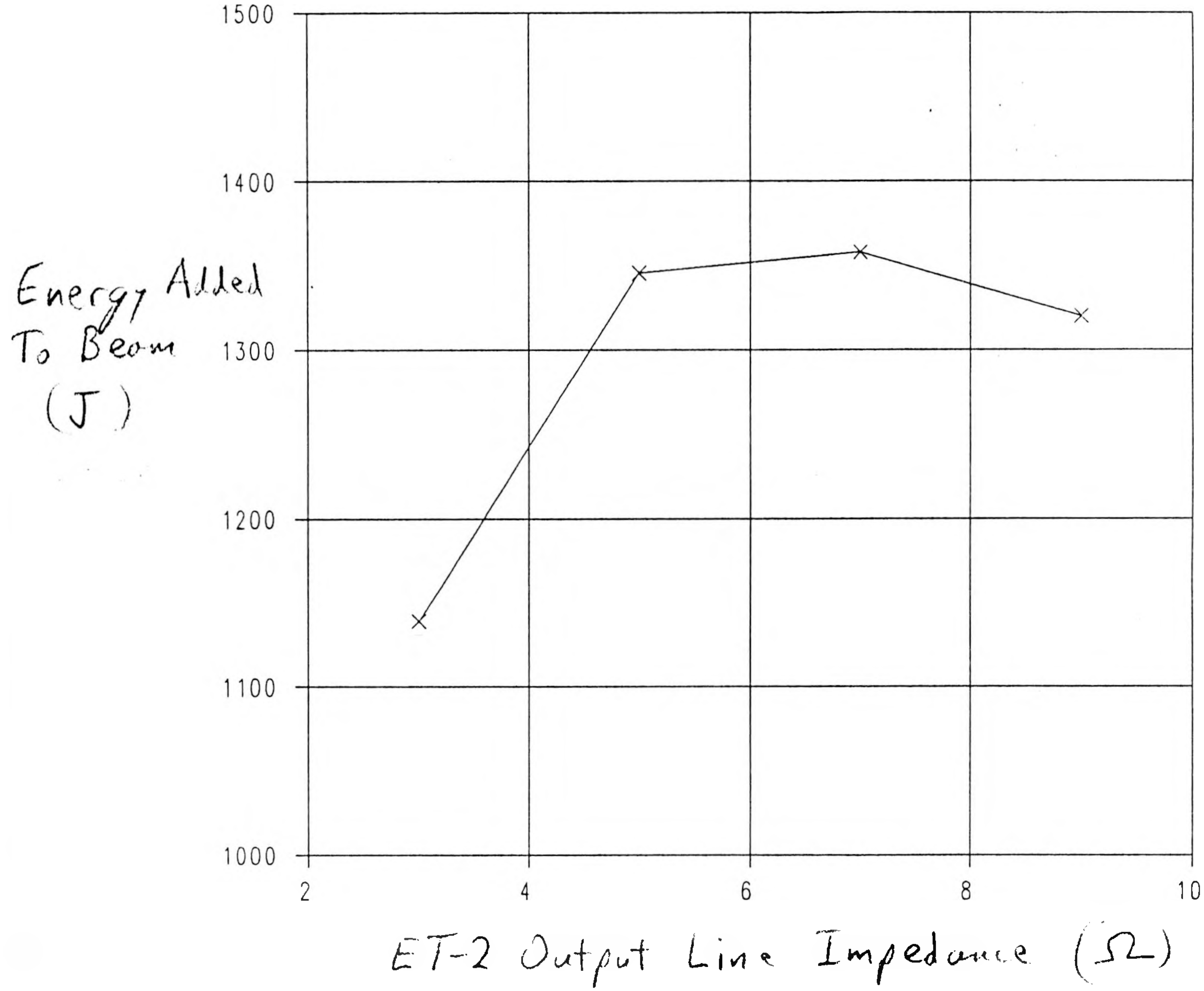

Fig. 2D

IIB3

THE SWITCH INDUCTANCE AFFECTS THE RISE TIME, AMPLITUDE, AND PHASE OF THE RINGING WAVEFORM

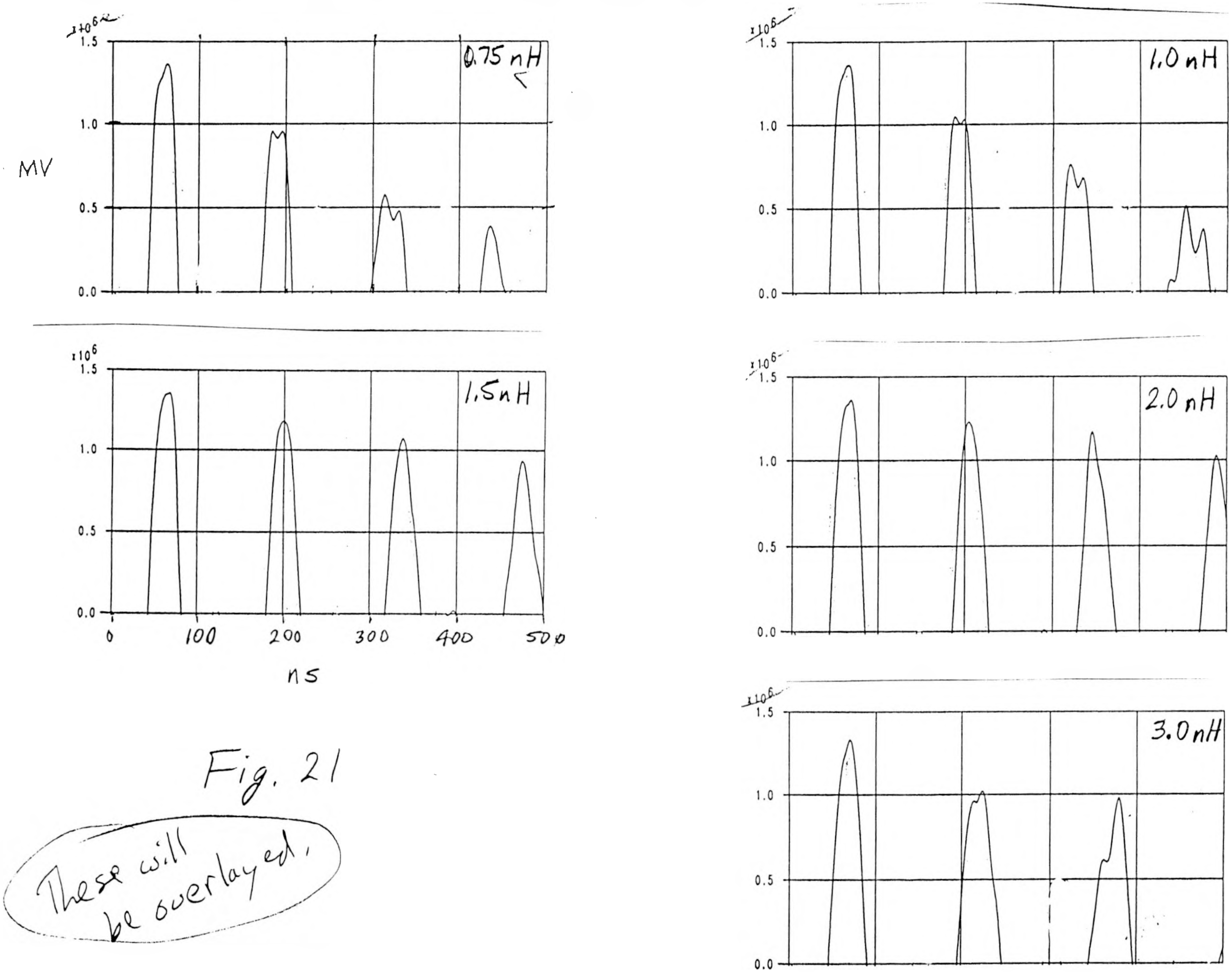

Fig. 21

These will be overlayed.

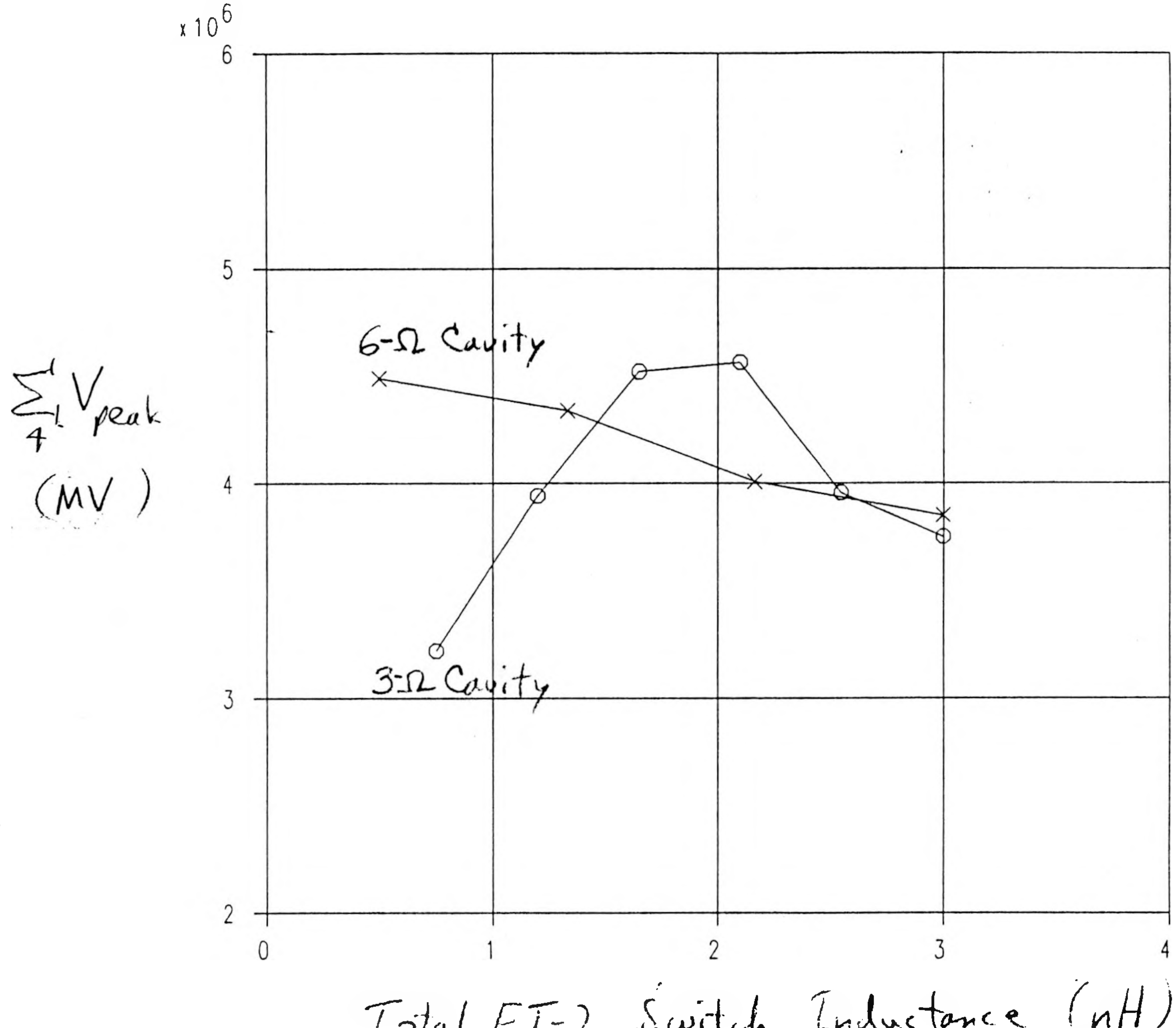
x 10^6
6
5
4
3
2
0
1
2
3
4
6-Ω Cavity
3-Ω Cavity
∑ V peak
(MV)
Total ET-2 Switch Inductance (nH)

Fig. 22

5/29/90 8:39:34

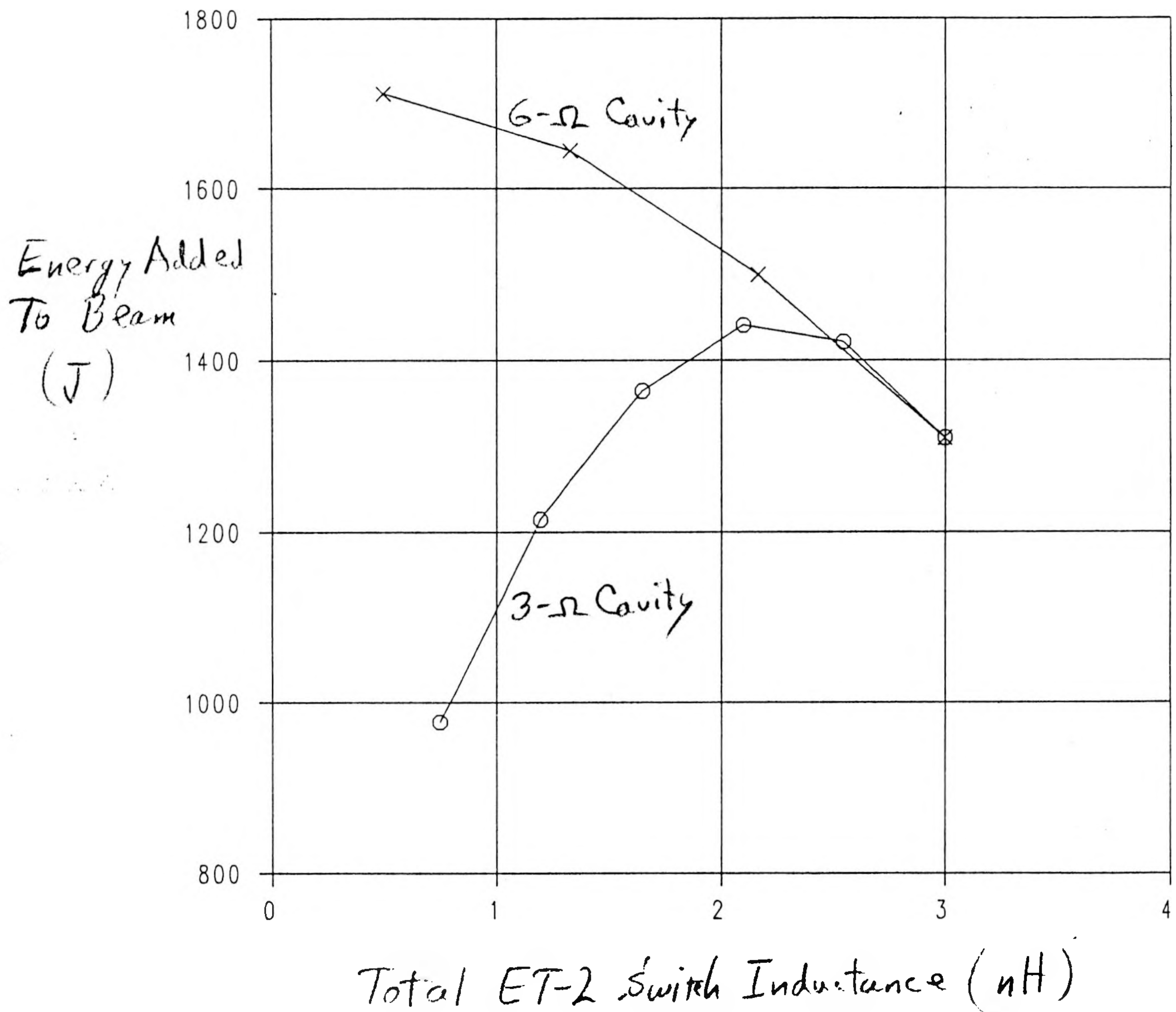

Fig. 23

IV B4

THE RADIAL 1.2(Split) . 6 Ω ET-2 ~~[illegible]~~ CAVITY 3 May 74 (2)
OPTION HAS SOME SYMMETRY ADVANTAGES
BUT ALSO OPERATIONAL DIFFICULTIES IV C

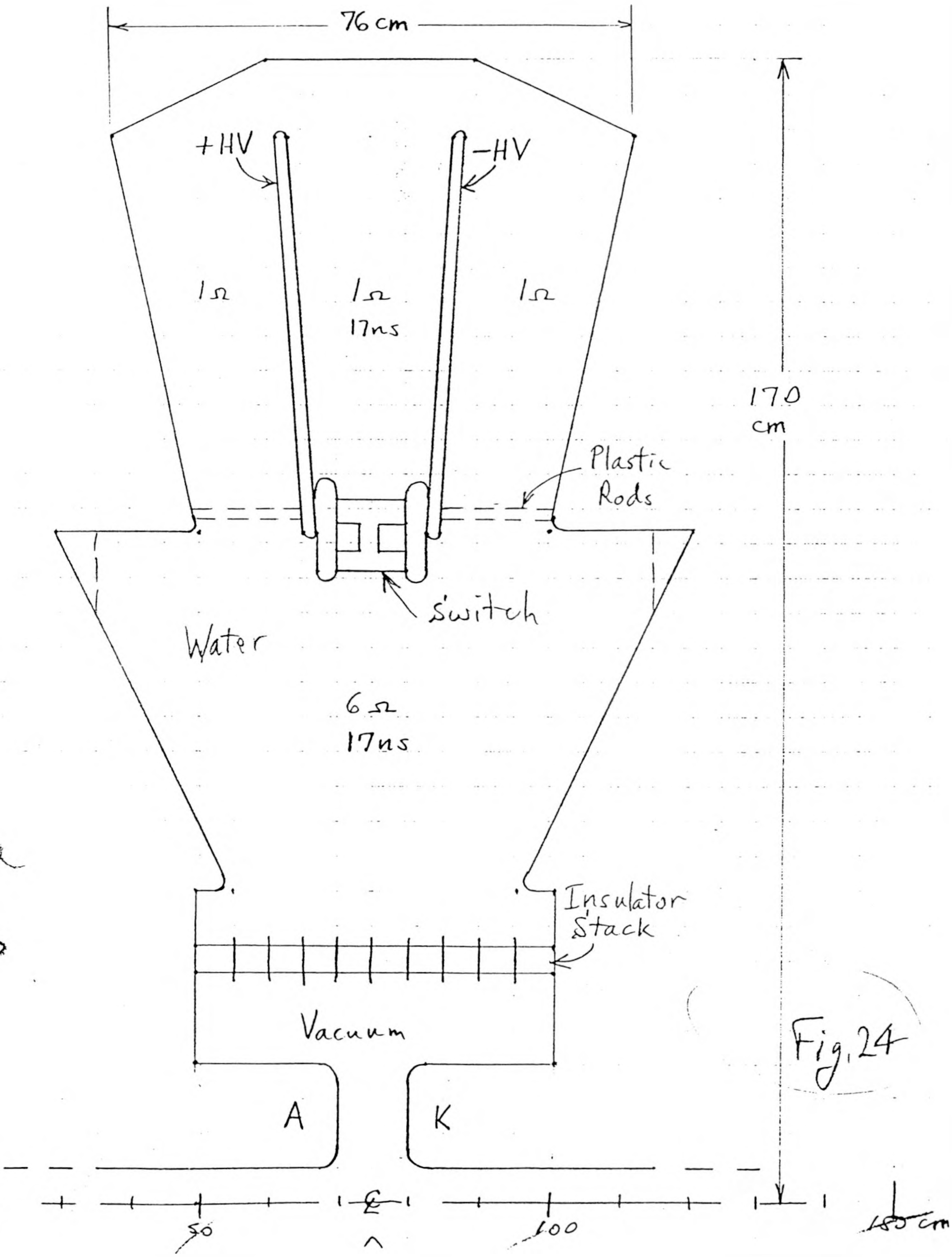

Fig. 24